



Calhoun: The NPS Institutional Archive DSpace Repository

Theses and Dissertations

1. Thesis and Dissertation Collection, all items

1975

Experimental investigation of the starting process of short diffusers for gas dynamic lasers.

Oudekerk, Milford Merwin

<http://hdl.handle.net/10945/20855>

Downloaded from NPS Archive: Calhoun



<http://www.nps.edu/library>

Calhoun is the Naval Postgraduate School's public access digital repository for research materials and institutional publications created by the NPS community.

Calhoun is named for Professor of Mathematics Guy K. Calhoun, NPS's first appointed -- and published -- scholarly author.

Dudley Knox Library / Naval Postgraduate School
411 Dyer Road / 1 University Circle
Monterey, California USA 93943

EXPERIMENTAL INVESTIGATION OF THE
STARTING PROCESS OF SHORT DIFFUSERS
FOR GAS DYNAMIC LASERS

Milford Merwin Oudekerk

DUDLEY KNOX LIBRARY
NAVAL POSTGRADUATE SCHOOL
MONTEREY, CALIFORNIA 93943

NAVAL POSTGRADUATE SCHOOL

Monterey, California



THESIS

EXPERIMENTAL INVESTIGATION
OF THE STARTING PROCESS OF SHORT DIFFUSERS
FOR GAS DYNAMIC LASERS

by

Milford Merwin Oudekerk
Lieutenant Commander, United States Navy
B.S., Naval Postgraduate School, 1971

June 1975

Thesis Advisor:

O. Biblarz

Approved for public release; distribution unlimited.

T168493

REPORT DOCUMENTATION PAGE		READ INSTRUCTIONS BEFORE COMPLETING FORM
1. REPORT NUMBER	2. GOVT ACCESSION NO.	3. RECIPIENT'S CATALOG NUMBER
4. TITLE (and Subtitle) Experimental Investigation of the Starting Process of Short Diffusers for Gas Dynamic Lasers		5. TYPE OF REPORT & PERIOD COVERED Master's Thesis June, 1975
7. AUTHOR(s) Milford Merwin Oudekerk Lieutenant Commander, United States Navy		6. PERFORMING ORG. REPORT NUMBER
9. PERFORMING ORGANIZATION NAME AND ADDRESS Naval Postgraduate School Monterey, California 93940		10. PROGRAM ELEMENT, PROJECT, TASK AREA & WORK UNIT NUMBERS
11. CONTROLLING OFFICE NAME AND ADDRESS Naval Postgraduate School Monterey, California 93940		12. REPORT DATE June, 1975
		13. NUMBER OF PAGES
14. MONITORING AGENCY NAME & ADDRESS (if different from Controlling Office) Naval Postgraduate School Monterey, California 93940		15. SECURITY CLASS. (of this report) Unclassified
		15a. DECLASSIFICATION/DOWNGRADING SCHEDULE
16. DISTRIBUTION STATEMENT (of this Report) Approved for public release; distribution unlimited.		
17. DISTRIBUTION STATEMENT (of the abstract entered in Block 20, if different from Report)		
18. SUPPLEMENTARY NOTES		
19. KEY WORDS (Continue on reverse side if necessary and identify by block number)		
20. ABSTRACT (Continue on reverse side if necessary and identify by block number) The diffuser section of a Gas Dynamic Laser (GDL) is one of the largest components in the system. The purpose of this investigation was to examine the problem of starting supersonic flow in short diffusers with fixed walls, incorporating various bleed arrangements for boundary layer control (BLC). A Mach number of 4, ramp angle of 19°, diffuser length of 4.5 inches and a diffuser width of 1.0		

inch were used throughout this investigation.

Intrusion by the atmosphere into the diffuser causes a separation region or "bubble" to form. The presence of this "bubble" could be made to improve the diffuser performance by making a variable area diffuser out of a fixed wall diffuser without the use of any external apparatus.

BLC was helpful in increasing the over all pressure recovery of the diffuser. BLC also affects the unsteady flow, which was present in the diffuser, but only when it is applied at a point prior to the converging section of the GDL.

Experimental Investigation
of the Starting Process of Short Diffusers
for Gas Dynamic Lasers

by

Milford Merwin Oudekerk
Lieutenant Commander, United States Navy
B.S., Naval Postgraduate School, 1971

Submitted in partial fulfillment of the
requirements for the degree of

MASTER OF SCIENCE IN AERONAUTICAL ENGINEERING

from the

NAVAL POSTGRADUATE SCHOOL
June 1975

ABSTRACT

The diffuser section of a Gas Dynamic Laser (GDL) is one of the largest components in the system. The purpose of this investigation was to examine the problem of starting supersonic flow in short diffusers with fixed walls, incorporating various bleed arrangements for boundary layer control (BLC). A Mach number of 4, ramp angle of 19° , diffuser length of 4.5 inches and a diffuser width of 1.0 inch were used throughout this investigation.

Intrusion by the atmosphere into the diffuser causes a separation region or "bubble" to form. The presence of this "bubble" could be made to improve the diffuser performance by making a variable area diffuser out of a fixed wall diffuser without the use of any external apparatus.

BLC was helpful in increasing the over all pressure recovery of the diffuser. BLC also affects the unsteady flow, which was present in the diffuser, but only when it is applied at a point prior to the converging section of the GDL.

TABLE OF CONTENTS

I.	INTRODUCTION -----	8
II.	STATE OF KNOWLEDGE OF SUPERSONIC DIFFUSERS --	9
III.	EXPERIMENTAL PROGRAM -----	11
	A. GENERAL -----	11
	B. TEST APPARATUS -----	12
	C. INSTRUMENTATION -----	13
IV.	EXPERIMENTAL INVESTIGATION -----	15
	A. GENERAL PROCEDURE -----	15
	B. FAST START MODE -----	16
	1. Pressure-Time Histories -----	16
	2. Schlieren Photography -----	18
	3. High Speed Photography -----	19
	C. SLOW START MODE -----	21
V.	START/FLOW MODEL -----	21
VI.	SUMMARY AND CONCLUSIONS -----	23
VII.	RECOMMENDATIONS -----	27
	DRAWINGS AND PHOTOGRAPHS -----	28
	APPENDIX A CALCULATION OF SHOCK WAVE SYSTEM -----	50
	APPENDIX B PRELIMINARY DESIGN CALCULATIONS -----	53
	APPENDIX C CALCULATION OF FRICTION FACTOR -----	56
	LIST OF REFERENCES -----	57
	INITIAL DISTRIBUTION LIST -----	59

LIST OF FIGURES

1. Drawing of basic GDL.
2. Photograph of test apparatus.
3. Diagram of NPS blow down wind tunnel.
4. Photograph of test section.
5. Diagram of Mach 4 nozzle vanes.
6. Photograph of high speed photography system.
7. Diagram of Schlieren system.
8. Cavity pressure-time trace without BLC.
9. Cavity pressure-time trace with BLC at point 2.
10. Cavity pressure-time trace with BLC at point 1.
11. Schlieren photograph without BLC.
12. Schlieren photograph with BLC at point 2.
13. Schlieren photograph with BLC at point 1.
14. Schlieren photograph with BLC at points 1 and 2.
15. High speed photograph sequence of the unsteady condition inside the diffuser. (bottom half of test section)
16. High speed photograph sequence of the unsteady condition inside the diffuser. (top half of test section)
17. High speed photograph sequence of the steady state condition inside the diffuser.
18. High speed shadowgraph of "bubble".
- 18a. Line trace of shadowgraph.
19. Diagram of "bubble" concept.
20. High speed shadowgraph sequence of the start process in the diffuser.

ABBREVIATIONS

ft	feet
lbm	pound-mass
sec	second
GDL	Gas Dynamic Laser
psia	pounds per square inch absolute
psig	pounds per square inch gauge
BLC	boundary layer control
CFM	cubic feet per minute
f	friction factor
M	Mach number
T	temperature ($^{\circ}$ R)
L	length
P	pressure
D	hydraulic diameter

I. INTRODUCTION

A considerable amount of experimental work aimed at reducing the total pressure losses in supersonic diffusers can be found in the literature today. Recent interest in gas dynamic and chemical lasers has spurred many new research projects within the past few years in the area of supersonic diffuser performance.¹

A typical gas dynamic laser (GDL) is shown in Fig. 1. As is evident in the figure, the diffuser section is by far the largest component. It has been the goal of research projects to reduce the size of this section for obvious reasons, such as lighter weight and faster starting.

Extensive work was done in the area of supersonic wind tunnel starting after World War II and into the early 1950's. Since the diffuser starting problem is similar to that of starting supersonic wind tunnels, a correlation can be quite easily made between the two. The obvious means which have been utilized in starting these tunnels are variable area diffusers, over-pressure, perforated walls, auxiliary air injection, and boundary layer control (BLC).²

The actual starting process of the diffuser begins with a normal shock wave traveling through the cavity and diffuser section. This normal wave is then reflected to some extent, but for the most part passes through the diffuser. A shock wave pattern then begins to form in the

cavity section. As this shock wave system moves downstream to the diffuser section, intrusion by the atmosphere begins at the downstream end of the diffuser and moves upstream, causing a separation region or "bubble" to form on the side walls. This separation region is pseudo-stationary in the sense that it oscillates at repeated frequencies; these appear to be eliminated by the appropriate use of BLC. When the shock wave system and the "bubble" come in contact with each other, an oblique shock wave, an expansion wave and a second oblique shock wave form, in that order, extending downstream. The actual location of this system will be discussed in detail in Section V. The words 'starting process' will refer to the wave formation that occurs after the initial normal shock wave has passed and the intrusion of the atmosphere into the diffuser section begins.

II. STATE OF KNOWLEDGE OF SUPERSONIC DIFFUSERS

Experimental work has been done which defines general design criteria for a supersonic diffuser and shows that supersonic diffusers may be divided into two main sections¹. These are, specifically, a convergent section to reduce the Mach number to some low supersonic value and a constant area section which further diffuses the flow to subsonic through friction and a shock wave system. The convergent section normally consists of a straight ramp whose angle is made small to inhibit shock-induced boundary layer separation in the region where the leading-edge shocks reflect

off the compression surfaces.

Experimental results show that increasing the diffuser contraction ratio beyond a certain maximum value results in "unstarting" (that is, the loss of supersonic flow within the diffuser).¹ Another significant experimental result is that removal of some or all of the low momentum boundary layer results in improved total pressure recovery. This is usually achieved by either a compression surface, or sidewall bleed, or by a combination of both.

Since total pressure losses in diffusers are produced by shock waves and by boundary layers, it is important to be able to estimate the magnitude, and hence the contribution towards total pressure loss of both of these effects in different parts of the diffuser.

It is well known that in order to establish supersonic flow in a fixed-throat diffuser, the contraction ratio of the diffuser can not exceed about 1.5 for an inlet Mach number of 4 to 5.³ Since for most applications the diffuser performance is inadequate for this contraction ratio, other means of starting diffusers have been used. The diffuser throat is frequently made part of a movable wall which is initially opened sufficiently to permit the starting wave system to be swallowed. The throat is subsequently closed to give the required Mach number in the throat region.

The object of the present work was to study the starting phenomena for fixed sidewall diffusers. A "bubble" formation model will be developed which shows the contribution

(or hindrance) of boundary layer control at various regions in the diffuser and the effect of diffuser length.

III. EXPERIMENTAL PROGRAM

A. GENERAL

In 1973, a research program was initiated at the Naval Postgraduate School, under NAVAIR sponsorship, to investigate diffuser performance. The program has thus far entailed two theses, one⁴ which explored various diffuser geometries and start up times, and another⁵ (a computer analysis) which looked at the unsteady flow problem associated with starting phenomena in various nozzle short diffuser combinations. The investigation accomplished in Ref. 4 indicates that diffuser performance is a function of diffuser length, width and ramp angle among other things. Pressure recovery was strongly dependent on diffuser length. For short diffusers, there was a general tendency to achieve the optimum pressure recovery using a ramp angle of 19° at Mach 4. On the other hand, for longer diffusers (greater than 8 inches in this case) the best pressure recovery was realized with a steeper ramp angle and a wider diffuser. The present work is a continuation of this program and reports the results of more extensive measurements on the start process of the diffuser section of a GDL using the Mach 4 flow with a 19° ramp.

The experiments were concerned with two separate areas of study: 1) a study of the pressure recovery and run times of the diffuser when various amounts of boundary

layer control were used, and 2) determination of a flow model for the starting process of supersonic diffusers.

B. TEST APPARATUS

Figures 2 and 3 show the test setup which consists of a supersonic wind tunnel with a bank of 4 nozzle vanes to simulate the flow conditions in a typical GDL. The flow channel (Fig. 4) was 4 inches by 1 inch in cross section and 8.5 inches long. Attached to the 1-inch side walls were two pieces of machined aluminum 5 inches long by 0.35 inches in depth with a 19° angle cut at one end to form the converging section of the diffuser. Machine tolerances were generally limited to within a few thousandths of an inch. The section of flow channel between the nozzle tips and start of the 19° ramp corresponds to a GDL cavity. Diffusion was limited to one dimension--there was no physical contraction of the 1-inch dimension. Optical quality glass windows extend from the nozzle tips to the flow exit plane, where the apparatus exhausts to the atmosphere.

Boundary layer control was in the form of suction, which was employed at two positions on one side of the apparatus only (see Fig. 4). Station one was located 5 inches from the nozzle tips. Station two was at the start of the 19° ramp 2.85 inches from the nozzle tips. Both stations consisted of a slit 0.1 inches wide by 1 inch long. Each station was equipped with its own shut-off valve, which allowed individual or simultaneous boundary layer control. The suction was accomplished through the use of an 18-inch

diameter bell jar which was evacuated by a 40-CFM ruffage pump. The pressure of suction used in all cases was 2 psia.

Figure 4 shows the test section configured for Mach 4 operation with a throat area of 0.126 square inches. Figure 5 shows a detail of the nozzle vanes.⁴

The Naval Postgraduate School Department of Aeronautics blow-down wind-tunnel facility served as the flow source. The facility provides dry air which can be regulated from 0 to 250 psig. In the transition section the flow cross section is transformed from circular, with a 4 inch radius, to rectangular, 4 inches by 1 inch. The transition is accomplished through an epoxy mold inside the 12-inch long section of pipe.

Typical mass flow and flow velocities were calculated to be 2.70 lbm/sec. and 9.1 ft/sec. respectively, prior to the nozzle area. The actual Mach number measured from Schlieren photographs in the test section was 3.99 to 4.02.⁴

C. INSTRUMENTATION

The actual experimental investigation was carried out utilizing three general methods of flow visualization: pressure-time histories, Schlieren photography, and high-speed shadowgraph photography.

High-speed photography was accomplished by the use of the model HS Fairchild 16mm high speed camera. Camera settings were as follows: f-stop 5.6, distance from subject 1.5 feet and camera speed 4800 frames per second. The film used throughout the experiment was Kodak 4-X Reversal 7277

in 400 foot lengths.

The light source for the high speed photography was provided by a high-efficiency, 2500 watt, xenon (Hanovia 975-C39) source from the Oriel Corporation. A light source of this type proved to be quite satisfactory as far as the actual high speed photography was concerned. However, there were several hazards associated with a source of this type which should be heeded by every user; they include: 1) eye hazard due to intense light radiation 2) hazard due to ozone 3) electrical shock hazard.⁶ Actual photography was accomplished by the setup shown in Fig. 6.

Still Schlieren photography was accomplished with the system shown in Fig. 7.

The pressure at location 4, was measured on a dial with a scale of 0 to 300 psig. Cavity pressure was measured on a dial with a scale of 0 to 25 psig connected into location 3. To record the pressure-time histories, the outputs from transducers at locations 3 and 4 were used alternately as the vertical inputs to a Tektronix 545 oscilloscope. The transducer at location 4 was a bourdon-tube type, 0 to 700 psig scale and 10,000 HZ frequency response. The location 3 transducer was the same type except the scale was 0 to 25 psig. A piezoelectric blast transducer at location 5 was fed through a charge amplifier to provide oscilloscope triggering.

IV. EXPERIMENTAL INVESTIGATION

A. GENERAL PROCEDURE

The general procedure throughout the experiment was the same, in that start and pressure recovery data were taken for the fast and slow start mode using the flow visualization methods mentioned previously.

The fast start mode consisted of a pressure rise from zero psig at location 4 of Fig. 3 to the desired test pressure in 0.1 seconds. In the slow mode the pressure was increased gradually in 5 psig increments to the desired test pressure.

Boundary layer control (BLC) was applied in this experimental investigation to determine what effect it would have on the starting of the diffuser. The BLC used in this experiment was in the form of suction at a pressure of 2 psia. All BLC was applied to the left side of the diffuser only (as one views the photographs). Reference points for the application of BLC are located at locations 1 and 2 of Fig. 3, which will be referred to from now on as location 1 or location 2.

The entire spectrum of data for this experiment was taken at least twice. The first series of data were taken using the Fisher Control Company's 310-32 gas regulator valve to regulate the flow in the Naval Postgraduate School blow-down wind-tunnel. With this valve incorporated in the system,

the start and recovery pressures were generally the same as the ones obtained in a previous experimental investigation.⁴

Diffuser start and pressure recovery data were then taken without the use of the gas regulator valve. This report will be concerned with the results of the data taken using this experimental setup.

B. FAST START MODE

1. Pressure-Time Histories

Cavity pressure-time history data were recorded for starting pressure from 91 psig to 190 psig using various applications of BLC. The pressure traces show that the start times were from 0.1 seconds to 0.17 seconds for pressures of 91 psig, regardless of BLC applications. The minimum starting pressure obtainable was 91.57 psig, which corresponds to the accepted values found in Fig. 5b, Ref. 3 for normal shock starting. The actual starting pressure was, in most instances, not a sharply defined point. Variations in the starting point between runs of up to 3.5 psig were noted throughout the experiment. For many of the conditions tested, the neighborhood of the starting point is characterized by oscillatory flow or by separated flow in the cavity. Errors in data reading may account for some of this scatter. Considering these conditions, it is felt that starting pressures determined are within an accuracy of \pm 3 psig.

The first pressure-time data taken were without the use of BLC. Operation in this mode allowed the diffuser to

start at a minimum pressure of 95 psig with a corresponding pressure in the cavity of 0.73 psig (see Fig. 8).

In an attempt to decrease the starting pressure, BLC was first applied at location 2, which is located at the base of the 19° ramp. Suction at this point allowed the diffuser to start and continue to run at a minimum pressure of 91.57 psig, with a pressure of 0.69 psig and with less pressure fluctuations in the cavity (see Fig. 9).

BLC was applied next at location 1, 5 inches downstream of the nozzle tips or 2 inches downstream of the 19° ramp. With BLC at this location, 106 psig was the minimum pressure obtainable in order that the diffuser would start and continue to run.

In still a further attempt to decrease the starting pressure, BLC was applied to both locations 1 and 2 simultaneously, in which case the minimum start and run pressure obtainable was 112 psig.

In order to obtain a better understanding of why the minimum start pressure increased when BLC was applied at location 1, a start pressure of 92 psig with suction at locations 1 and 2 was next used. The suction at location 1 was cycled on and off at 1-second intervals. As can be seen in Fig. 10, the use of suction at location 1 had the tendency to unstart the diffuser, then when suction was ceased, the diffuser restarted again, until suction was reapplied at location 1.

A possible explanation as to why BLC at location 1

increased the minimum starting pressure is that applying suction in this area removes the "bubble", which was referred to in Ref. 7. This bubble, which is clearly visible in the high speed photographs, is apparently beneficial to diffuser start and run. Removing the "bubble" by the use of suction decreases the overall performance of the diffuser and increases the minimum starting pressure.

2. Schlieren Photography

Schlieren photographs were taken at all data points in order to obtain a better idea of shock wave formation and Mach angle. Figure 11 shows a Schlieren photograph of the flow at 95 psig start pressure with no BLC. The Mach number was measured and found to be 4.0. As is evident in the photograph, the top of this picture, and all other Schlieren photographs, is completely "washed out". This washout phenomenon will be explained in the next section where high speed photography is discussed.

Boundary layer control of the same type used previously was incorporated again in order to obtain a better idea of its effect at various points in the diffuser. The first application of BLC was applied at location 2; the results are shown in Fig. 12 (BLC is on the left side as one looks at the picture). The Mach number was again measured and found to be 4.0. As should be evident in the photograph, the weak shocks starting on the left-hand side wall just below the ramp have been eliminated.

BLC was then applied at location 1. BLC in this

position seemed to have little or no effect on the flow (see Fig. 13). As can be seen in the photograph, the weak shocks on the left side of the diffuser just below the ramp are still visible just as they were when no BLC was used.

The third and final application of BLC consisted of suction at location 1 and 2 simultaneously. Figure 14 shows the results of this attempt at BLC. As was the case when BLC was used only at location 2, the shocks starting on the left-hand side wall (as one looks at the picture) seem to weaken if not disappear entirely.

As was seen in the pressure-time histories, suction at location 1 decreased the efficiency of the diffuser. Whereas when suction was applied at location 2, the efficiency of the diffuser seemed to increase, since the flow is unable to separate prior to the 19° ramp.

3. High-Speed Photography

High-speed photography in the form of 16mm motion pictures was used as a third means of flow visualization. This type of data acquisition allowed some understanding of the actual wave motion in the start and unstart process of the diffuser. Motion pictures were taken both with and without suction, at starting pressures of 91 psig to 190 psig.

A phenomenon of importance, that of the so-called "washout" mentioned in the previous section and in Ref. 4, can be explained through the use of these high speed motion pictures. This effect is caused by the shock waves moving back and forth across the diffuser at a rate of 1 inch per

millisecond. Figures 15 and 16 show a series of high speed motion picture frames taken at 4800 frames per second with a starting pressure of 91 psig with no BLC used. The sequence of pictures shows the actual wave motion inside the diffuser that causes this "washout" or unsteadiness observed previously in all Schlieren photographs.

When BLC was used at location 2 the unsteady flow vanished and the wave motion inside the diffuser became steady (see Fig. 17). BLC was also used at location 1 but, unlike the application of BLC at location 2, this did not help to steady out the flow. In fact it made the flow even more unsteady. BLC at locations 1 and 2 simultaneously had the same effect as when BLC was applied at location 1 only, in that the flow remained unsteady in the diffuser section.

High speed photography also allowed us to see the actual wave formation in the diffuser section (see Fig. 18, 18a). This formation proves that the "bubble" mentioned previously and in Ref. 7, actually does exist. This "bubble", located on the left and right side walls, decreases the diffuser width by about one third, making a variable area diffuser out of a fixed wall diffuser without the use of any external apparatus. This decrease of the diffuser area improves the diffuser performance in this fixed wall diffuser, just as it does in the variable area diffuser. The actual "bubble" consists of air at atmospheric pressure entering at the exit of the diffuser and traveling down the diffuser

walls to a point just above the ramp section. Figure 19 shows a diagram of the "bubble" model.

C. SLOW START MODE

A slow start mode was used in an attempt to obtain a better understanding of the actual start process of the diffuser. In this mode, the pressure was gradually increased from zero to the starting pressure desired. It was observed in the high speed photography, Schlieren photographs and pressure-time histories, that once the starting pressure level was achieved the diffuser started in the same amount of time (0.1 seconds to 0.17 seconds) regardless of the rate of pressure increase. When this fact was discovered, further data using this mode was no longer pursued.

V. STARTING/FLOW MODEL

This section will attempt to tie together all previous sections of this report in order to obtain a precise description of the starting process of the diffuser section of a GDL.

Figure 20 shows a series of high speed 16mm pictures, which show in detail the actual wave formation inside the cavity and diffuser sections. As the pictures illustrate, the diffuser seems to start, that is, the shock waves begin to form on one side of the cavity wall and proceed downstream until Mach 4 flow is achieved. It is evident from this series of pictures, and numerous other 16mm films, that the "bubble" effect mentioned previously is present in

the start, also. As the diffuser starts, that is, after the initial normal shock wave passes through the cavity and diffuser section, intrusion of the atmosphere begins at the side walls. This intrusion is recirculating air, which enters the diffuser close to the side walls and proceeds upstream to some location where it is turned around and allowed to return downstream to a location where it can vent to the atmosphere.

The location of this "bubble" is of primary importance to the diffuser start sequence. The optimum location of the leading-edge of the "bubble" is at the end of the 19° ramp. It extends downstream to a point where the trailing edge can vent to the atmosphere at the end of the diffuser section. It was observed in high speed photography that deviations of the "bubble" from this position did not contribute to diffuser performance. If the leading edge of the "bubble" moved to a location upstream from this optimum position, the diffuser would not start. A possible explanation for this unstart condition is that the angle of the leading oblique shock, as shown in Appendix A, is too great, causing a decrease in the size of the actual throat area between the "bubbles", which causes a choked condition to occur. A movement in the downstream direction, however, did not contribute or hinder diffuser performance. Movement in this direction did not affect the leading oblique shock, thus the throat area was not decreased.

Appendix A shows calculations of the optimum position,

the upstream and downstream movement of the "bubble", and the shock wave system. As can be seen in these calculations the final pressure in all cases was 14.7 psi. The diffuser operates in such a way that this pressure must be achieved at the conclusion of the shock wave system. The bubble location and size seem to be determined by the position of this 14.7 psi pressure line.

VI. SUMMARY AND CONCLUSIONS

Currently one way to improve diffuser performance is to incorporate the use of movable walls. The present study indicates, however, that the formation of a separation region of "bubble", which generates itself in short diffusers, allows the fixed wall diffuser to operate as a variable area diffuser without having to use any external apparatus. Pressure recovery is considerably better than that for fixed wall, short diffusers.¹²

The final few paragraphs will list some of the factors that have led us to the conclusion of the existence of these "bubbles" and their importance.

1. A geometrical configuration of zero degree ramp, i.e., no wall contraction was used in Ref. 4, Fig. 28. Using this configuration the diffuser was still able to start and operate. This fact would seem to indicate that diffusion was made possible by contraction on the side walls through the presence of a "bubble".

2. The unsteady wave motion,¹⁷ which produced the "washout"

apparent in all Schlieren photographs, as well as other relevant times were at a rate which is much too slow to reflect the initial shock wave travel. It is more reasonable to conclude that the formation and collapse of the "bubble" produced the unsteady condition.

3. When BLC was applied at location 1 of Fig. 2, the diffuser would not start, or if it was started, it would unstart when BLC was reapplied at this location. This unstart condition was caused by removal of some or all of the bubble from the diffuser section.

4. All high speed photographs show clearly the existence of an area of recirculating, constant pressure flow along the diffuser side walls. As can be seen in the photographs, this flow extends from the end of the diffuser, where it is at atmospheric pressure, to some point upstream near the ramp section.

5. Appendix B shows a preliminary attempt at establishing a design criterion using the "bubble" concept. The Appendix shows a plot of P_t/P_a for various θ . This plot is a composite of data taken in Ref. 4, and of calculated values arrived at using the "bubble" model theory. In Ref. 4 the ramp angle (θ) was varied mechanically and P_t was measured directly in the laboratory. The second curve of Fig. 1B was calculated using the "bubble" model to determine P_t analytically, varying the ramp angle from 10° to 30° .

Considering that the two sets of data have some correlation, the "bubble" model for short diffusers appears to be

a realistic parameter which should be considered in short diffuser preliminary designs.

6. The location of the "bubble" proved to be of great importance in the start sequence, primarily because of the change in the second throat area, which resulted when the "bubble" was in various positions. If the "bubble" moved to a position upstream of the ramp, the second throat area between the "bubbles", on either side of the diffuser, decreased causing a choked condition which resulted in a no start sequence. On the other hand if the "bubble" moved to a position downstream of the ramp, increasing the throat area, the diffuser performance was not changed from that when the "bubble" was located at the end of the ramp. Therefore a "bubble" located at the start of the ramp proved to be optimum for start and run operation (see Appendix A) insofar as short length diffusers are concerned.

7. The fact that the final pressure in the diffuser was calculated to be 14.7 psi (see Appendix A) would tend to definitely prove that there is a recirculating area of atmospheric pressure in the diffuser section.

8. The calculation of a friction factor in Appendix C shows a correspondence to the theoretical curves for relatively smooth ducts found in Ref. 8. This fact would seem to indicate that one could use friction factors to describe the separated region inside the diffuser section.

9. When a centerbody was placed in the flow (see Fig. 24, Ref. 4) the pressure recovery in the diffuser decreased.

One reason for this decrease in performance might be that insertion of the centerbody interferes with the formation of the "bubble" and decreases the over-all diffuser performance.

In the diffuser design used in the present work the side wall, with BLC at location 2, acted as one half of a centerbody. However, the use of BLC allowed the diffuser to start and run with relatively good performance. Considering the above facts, it may be stated that diffuser configurations that include centerbodies should be designed for normal shock starting. By allowing the "bubble" to form in each section of the diffuser, the over-all diffuser performance would improve.

10. Reference 4, Figs. 28, 29,30, show that when P_t was increased from 55 psig to 65 psig the flow separated from both diffuser walls. It is now known that this separation is actually the formation of the recirculating area.

Finally, considering all the facts presented above, it is clear that the existence of a recirculating area of atmospheric pressure (or bubble) in short diffusers may be used to advantage.

VII. RECOMMENDATIONS

A continuation of the work in the area of short diffusers should be pursued at NPS. The high-intensity arc lamp and high speed camera are available and operational; the other, more conventional measurements are also at hand and operational. This work should include a study of the following areas:

1. Development of an accurate way to predict the shock wave system inside the diffuser using the "bubble" model technique.
2. Extensions of the work done in Ref. 4 on various diffuser geometries, incorporating the "bubble" condition and its effect.
3. Attempt to clean up the flow in order to eliminate the coalescing of the shocks prior to the ramp section in the test section.
4. More precise work in the area of friction factor determination. This work could be accomplished using high speed and Schlieren photography concentrated in the area where the formation of the "bubble" occurs.
5. Attempt diffusion on the glass side walls in order to offset the boundary layer growth.
6. Application of BLC in the area of nozzle wakes in order to eliminate their interference in the diffuser performance.

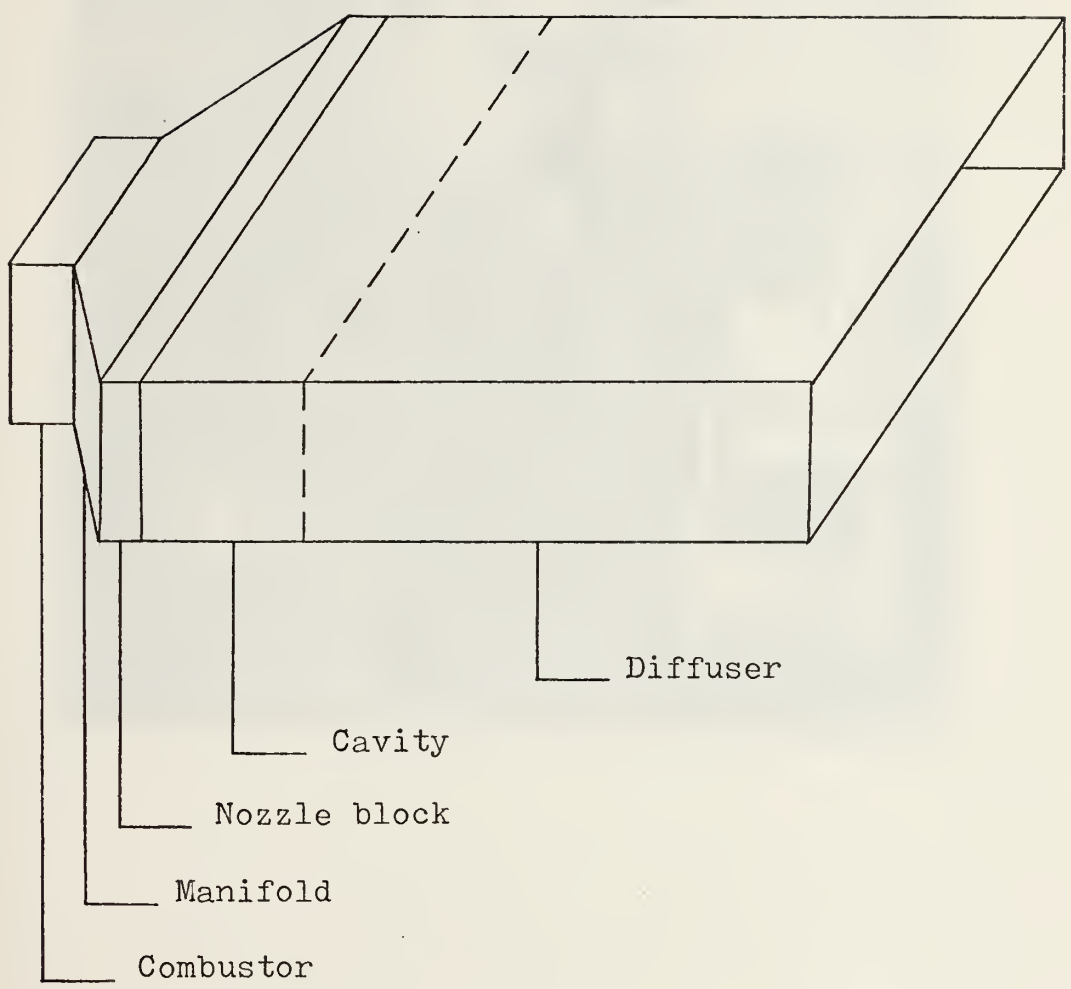


Figure 1. Schematic of basic GDL.

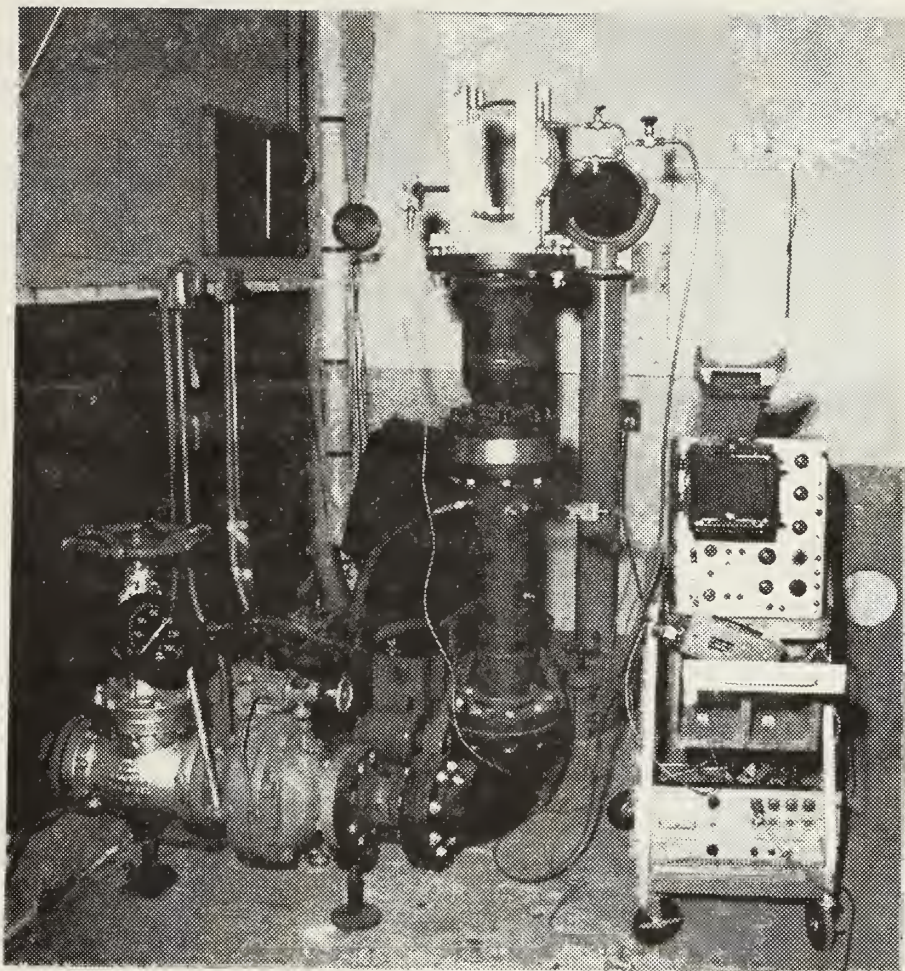


Figure 2. The NPS blow down wind tunnel with test section.

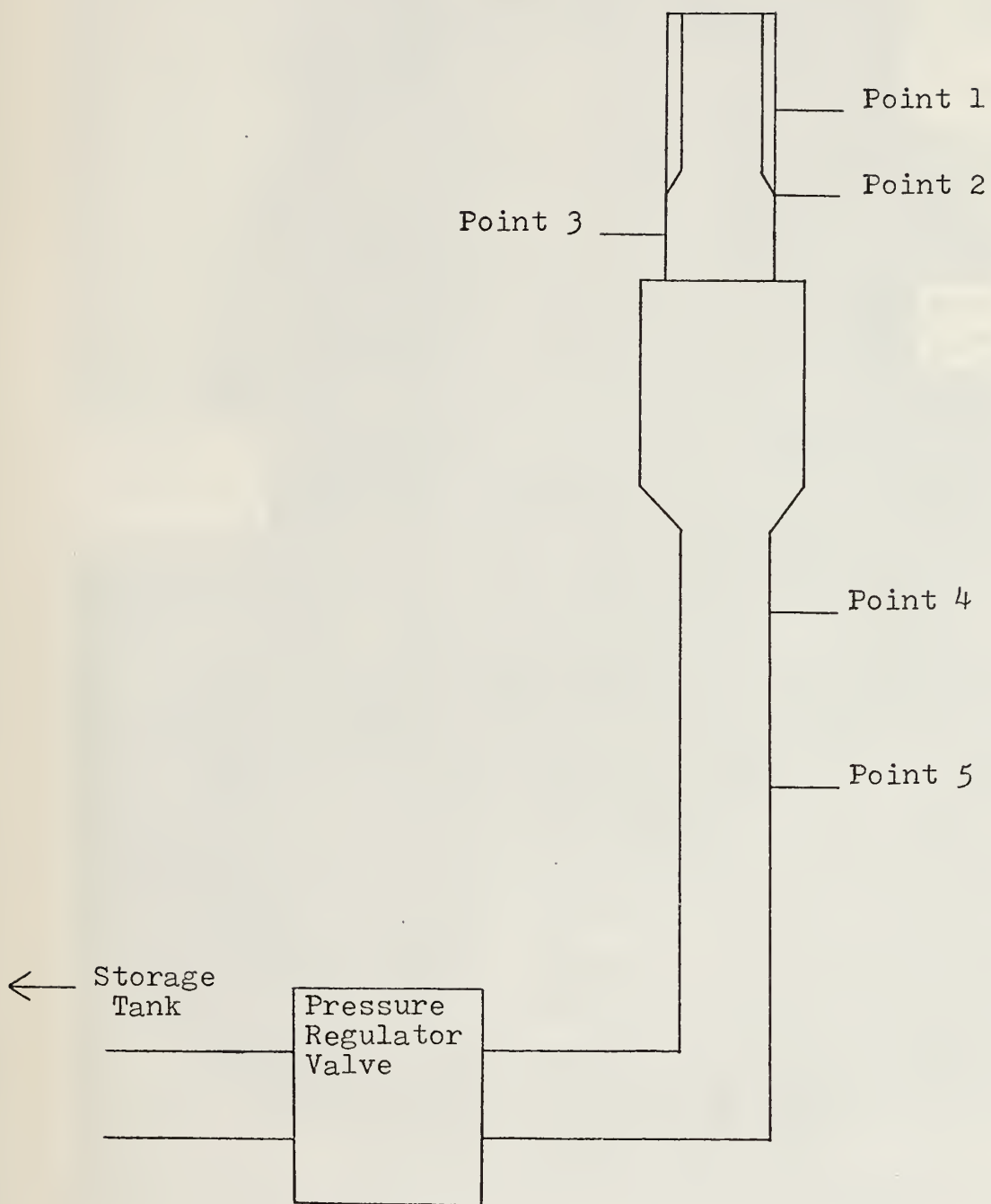


Figure 3. Experimental Set Up Showing the Location of Transducers Pressure Taps and BLC.

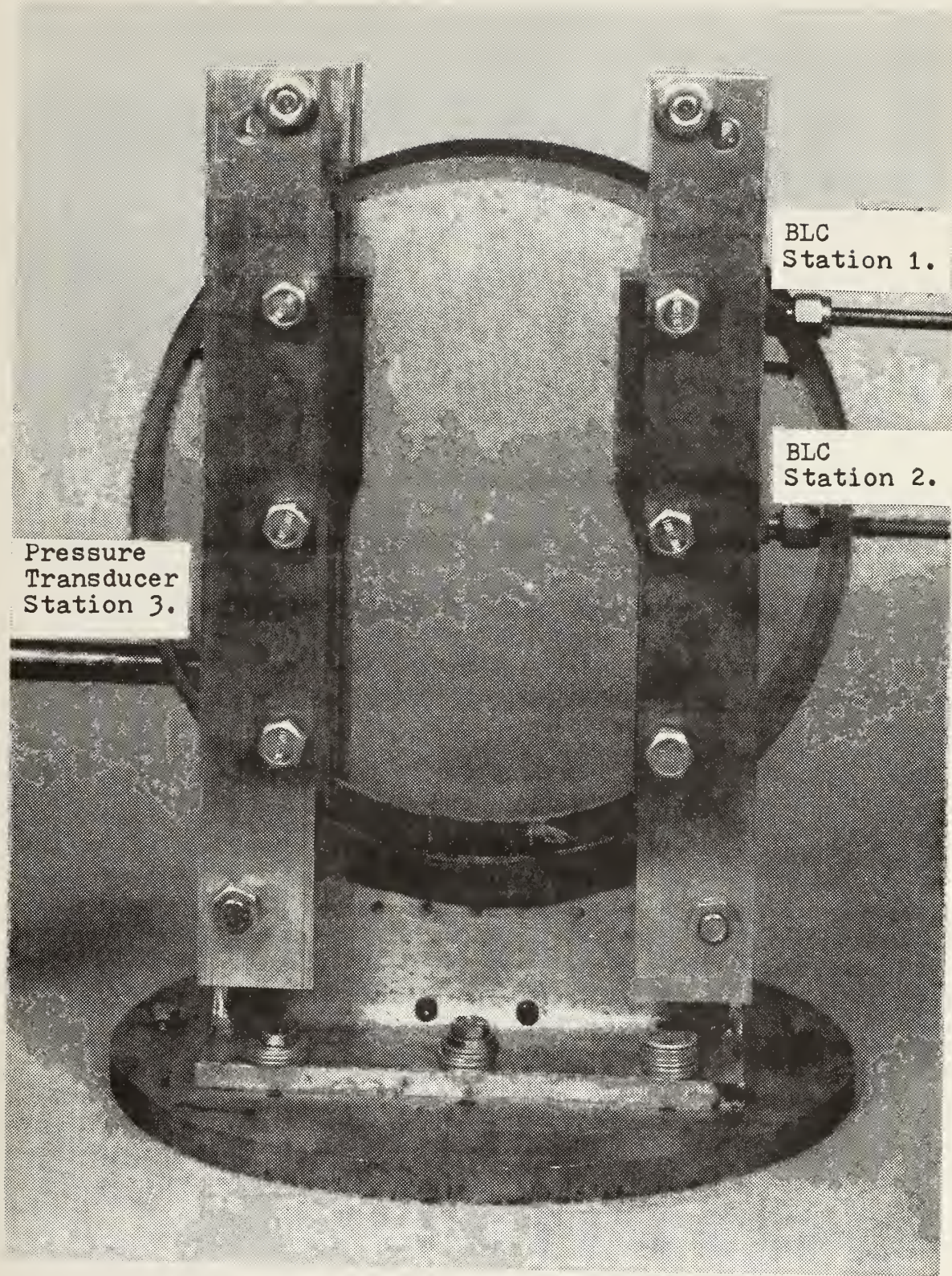


Figure 4. Closeup of Test Section.

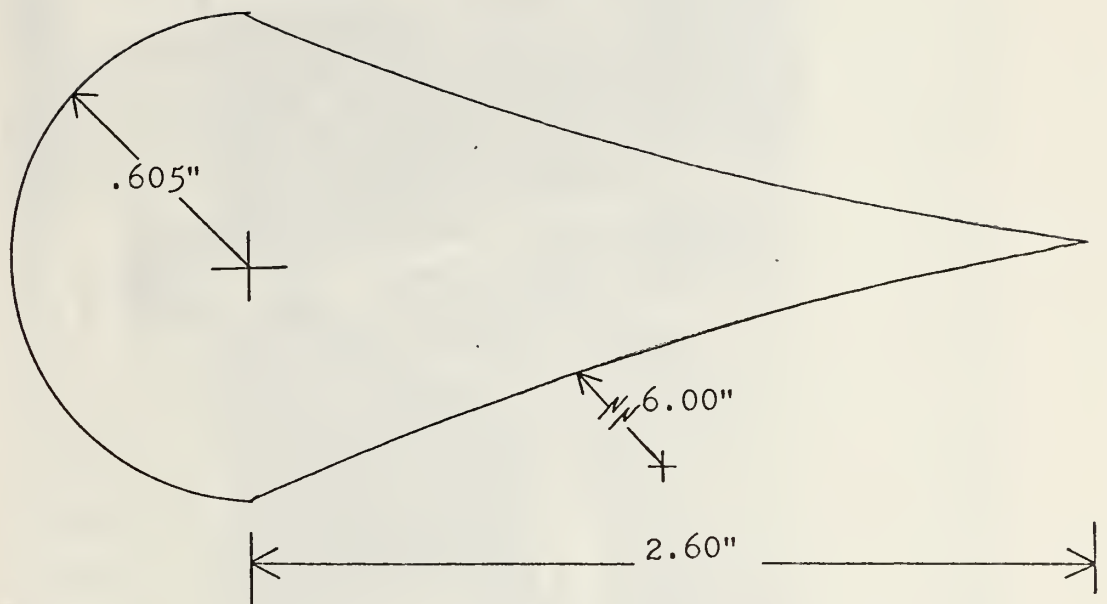


Figure 5. Mach 4 Nozzle Detail.

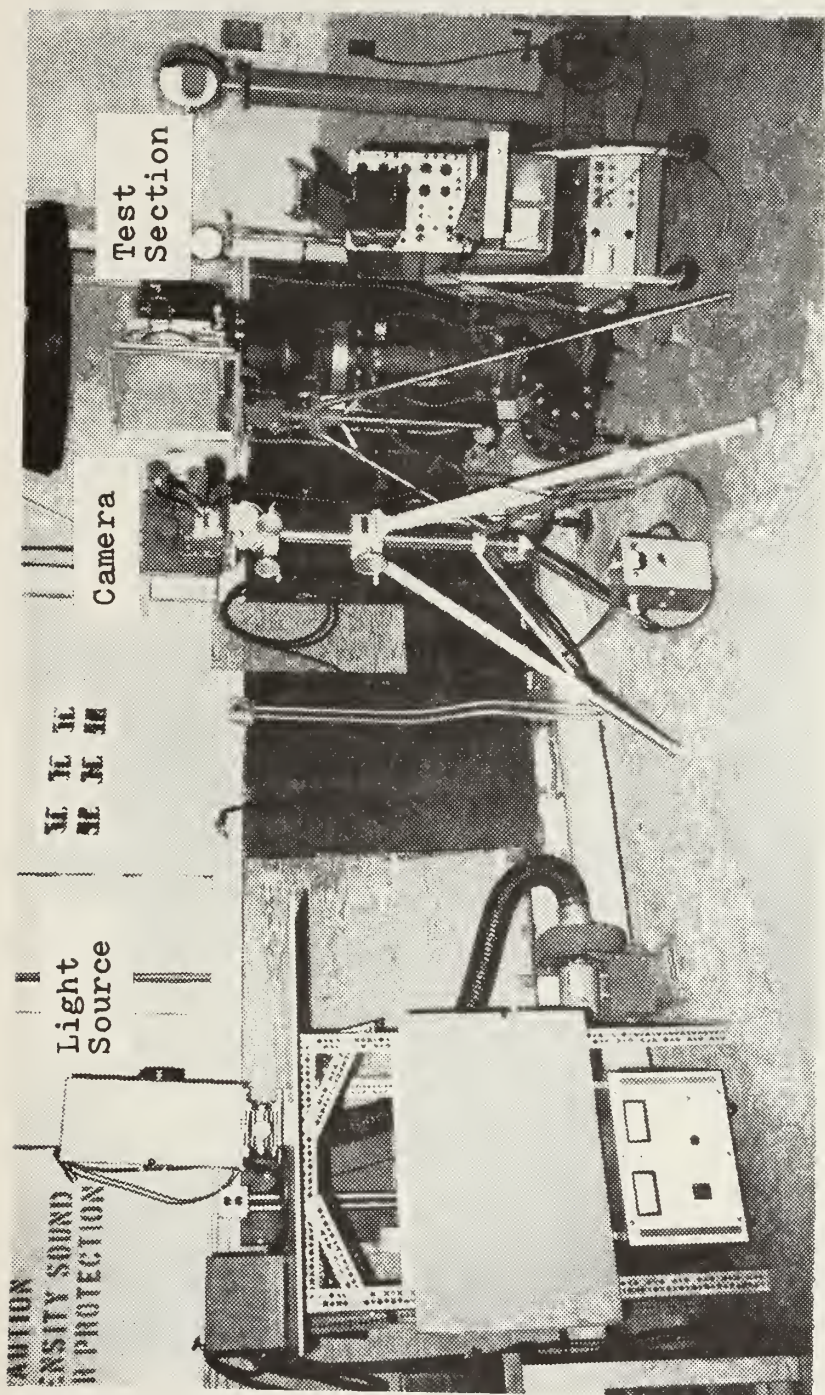


Figure 6. Experimental Set Up Showing High Speed Photographic Equipment.

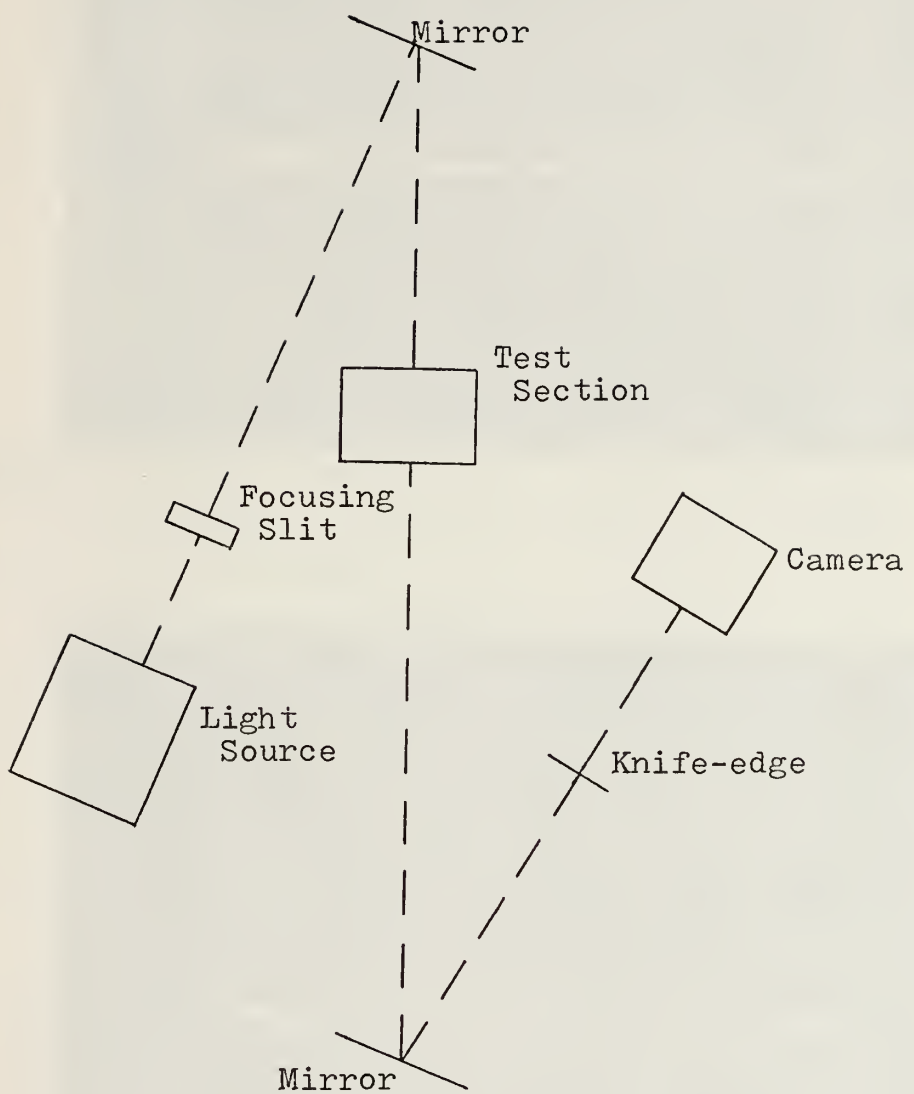


Figure 7. Diagram of Schlieren System.

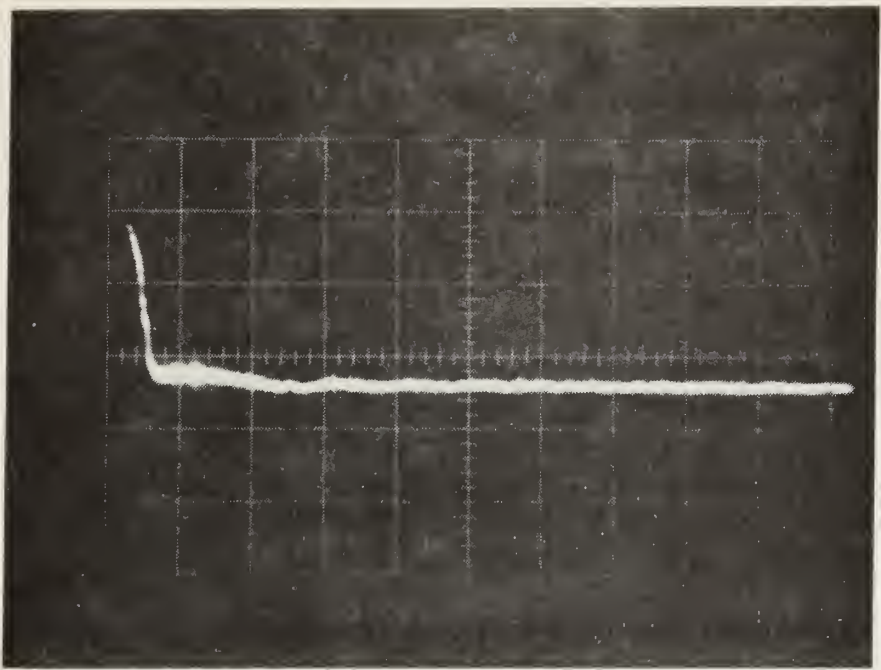


Figure 8. Cavity pressure-time trace without BLC.
Horizontal scale 0.5 sec./cm., Vertical
scale 2.0 volts/cm., conversion 1.0 volts
= 2.79 psig.

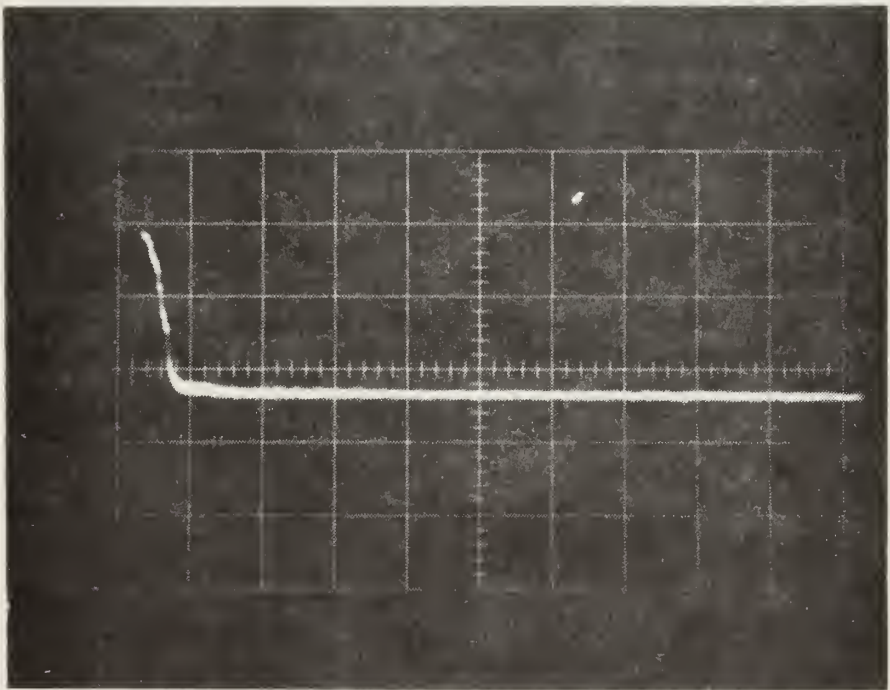


Figure 9. Cavity pressure-time trace with BLC applied
at location 2. Horizontal scale 0.5 sec./cm.
Vertical scale 2.0 volts/cm., conversion
1.0 volts = 2.79 psig.

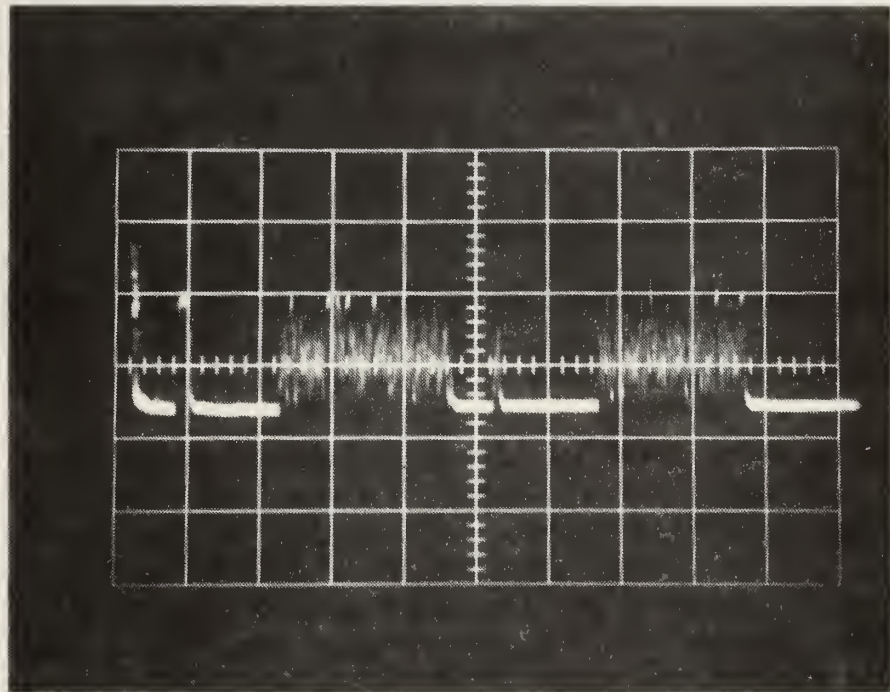


Figure 10. Cavity pressure-time trace with BLC at location 1 cycled on and off. Horizontal scale 0.5 sec/cm., Vertical scale 2.0 volts/cm., conversion 1.0 volts = 2.79 psig.

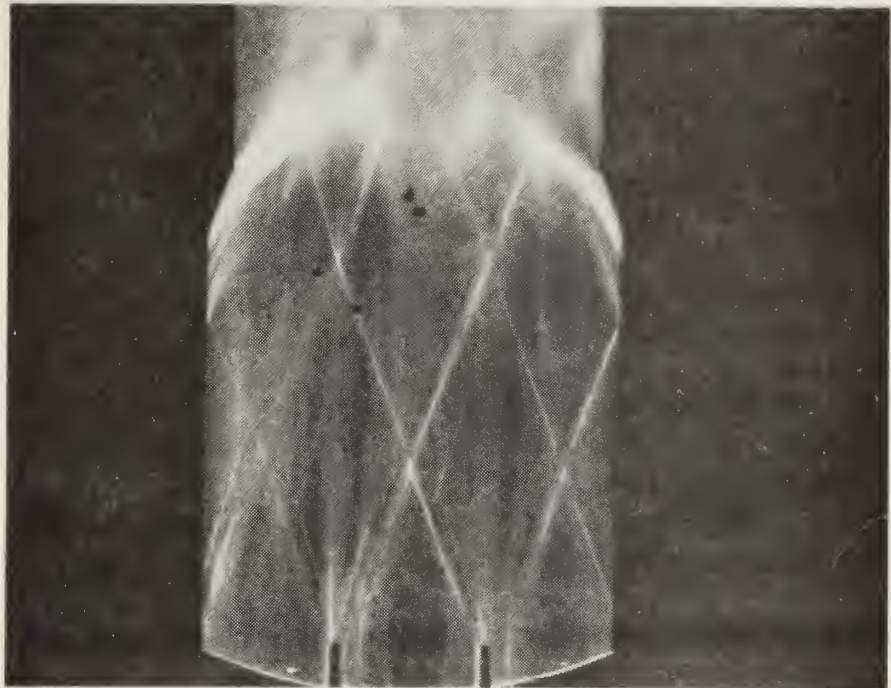


Figure 11. Schlieren with no BLC.



Figure 12. Schlieren with BLC applied at location 2.

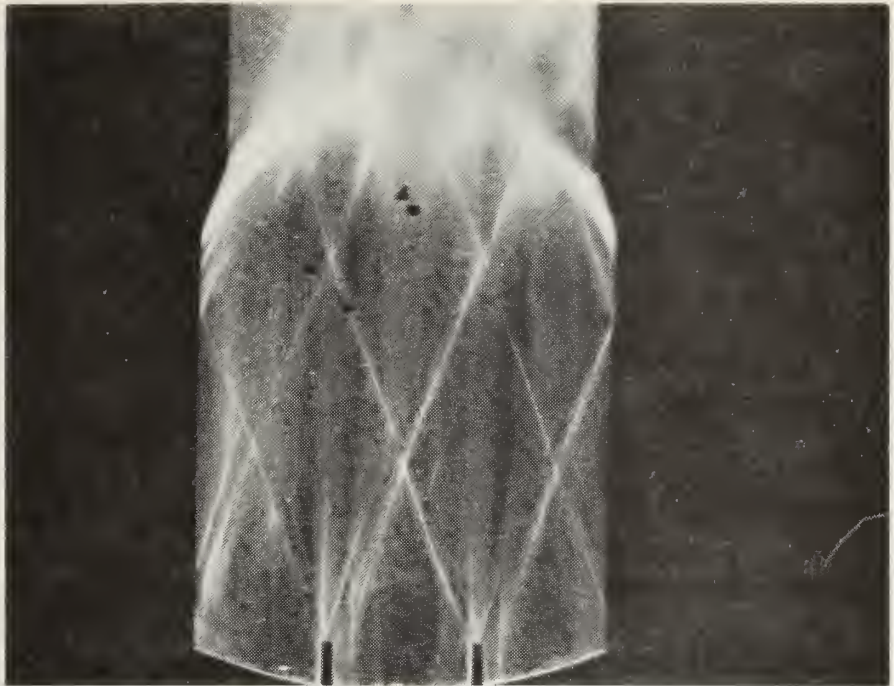


Figure 13. Schlieren with BLC applied at location 1.

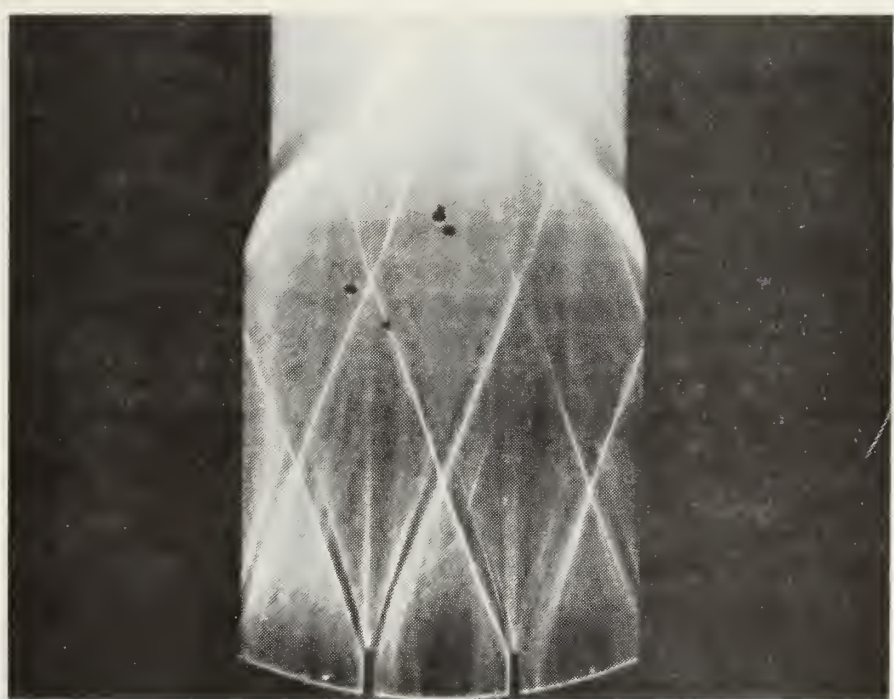
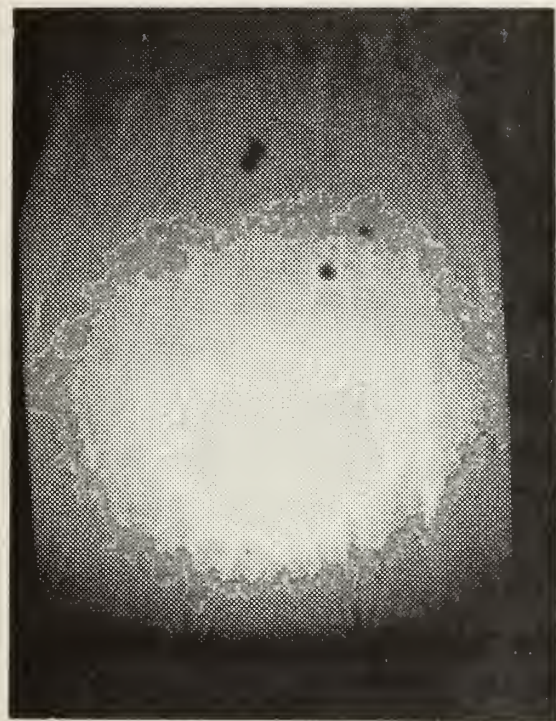
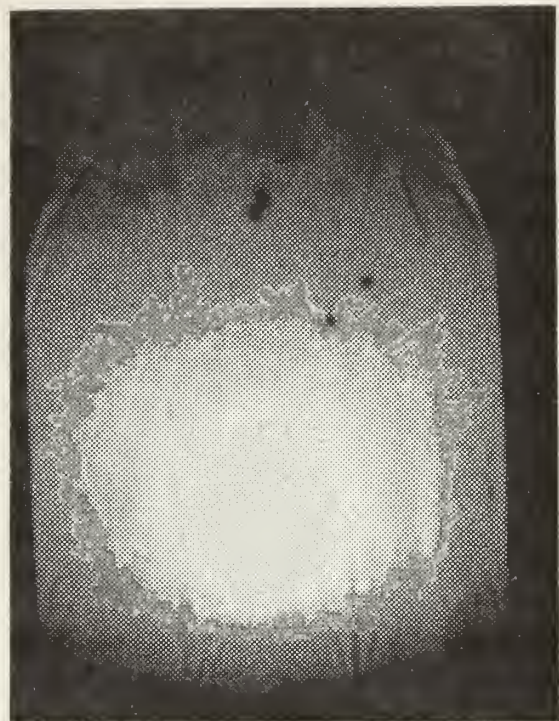


Figure 14. Schlieren with BLC applied at locations 1 and 2.



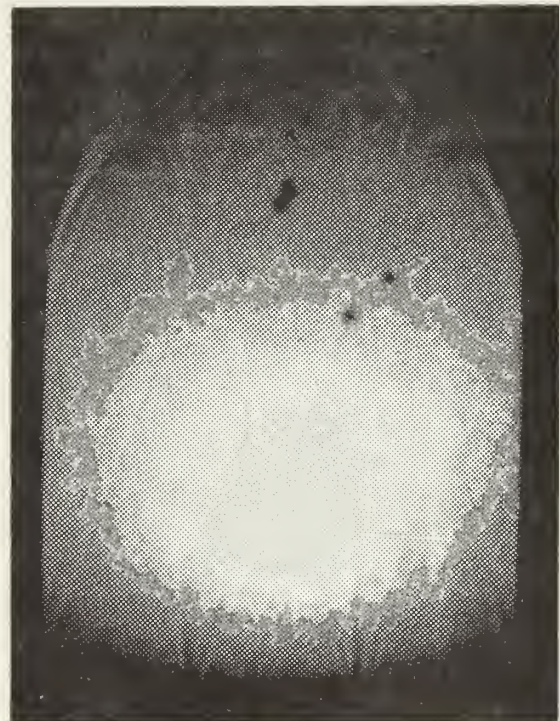
1



2

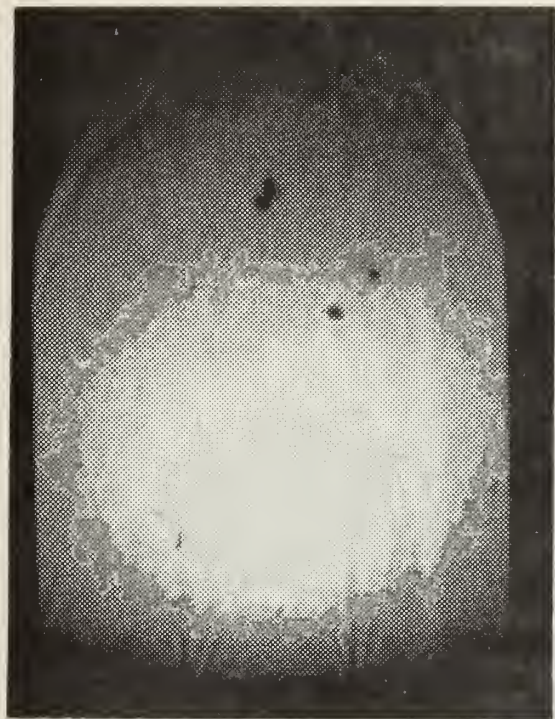


3

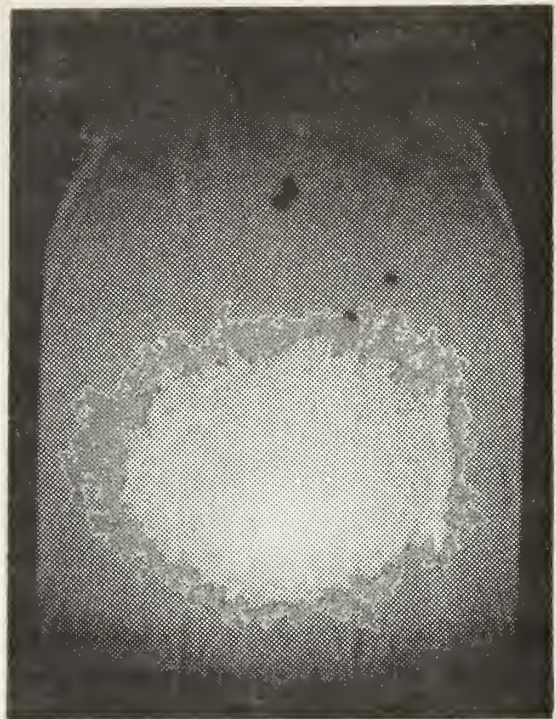


4

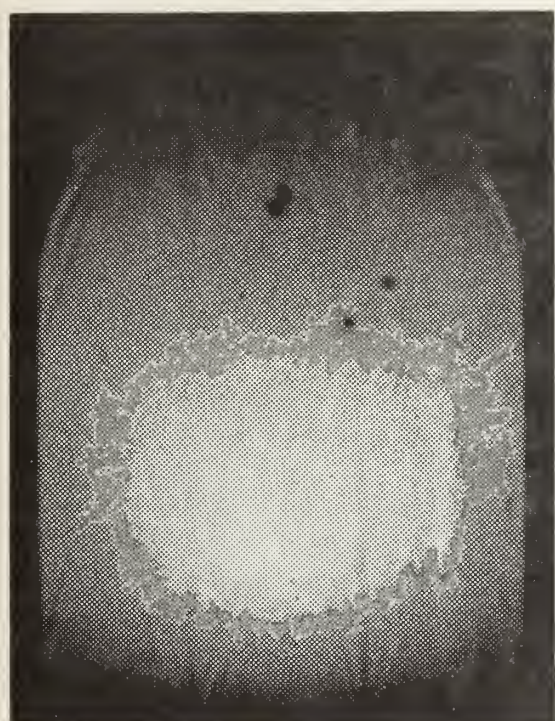
Figure 15. High speed sequence of unsteady condition.
(bottom half of test section)
Time between pictures in sequence 0.28 ms.



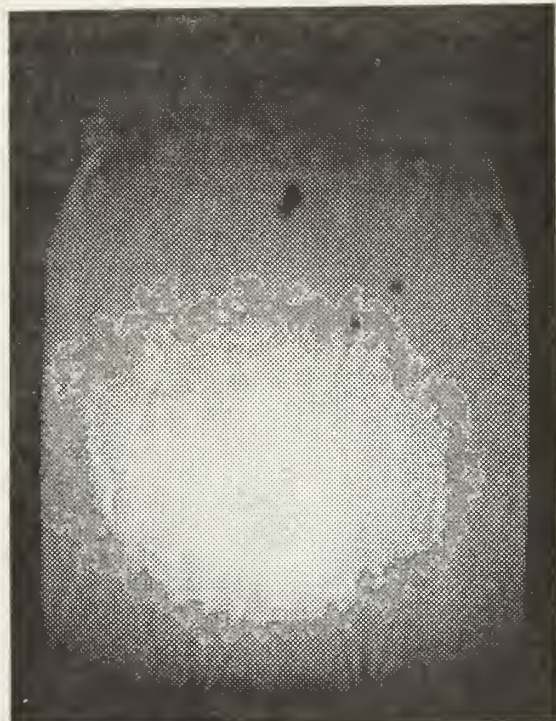
5



6



7



8

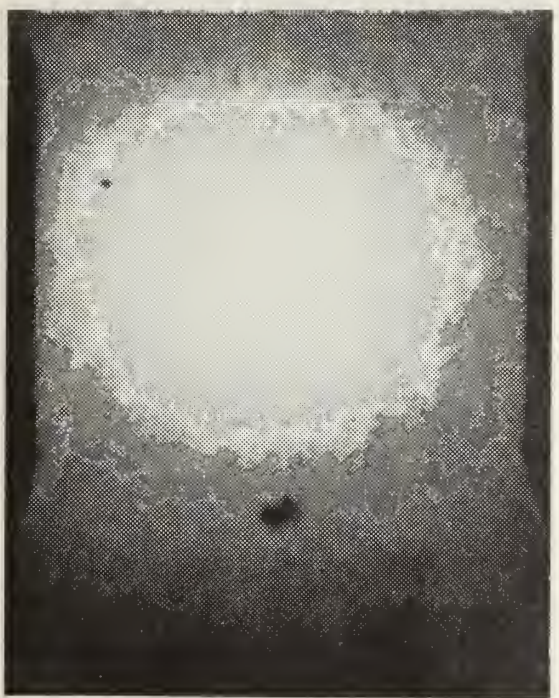
Figure 15. continued



1



2



3



4

Figure 16. High speed sequence of unsteady condition.
(top half of test section)
Time between pictures in sequence, 0.28 ms.



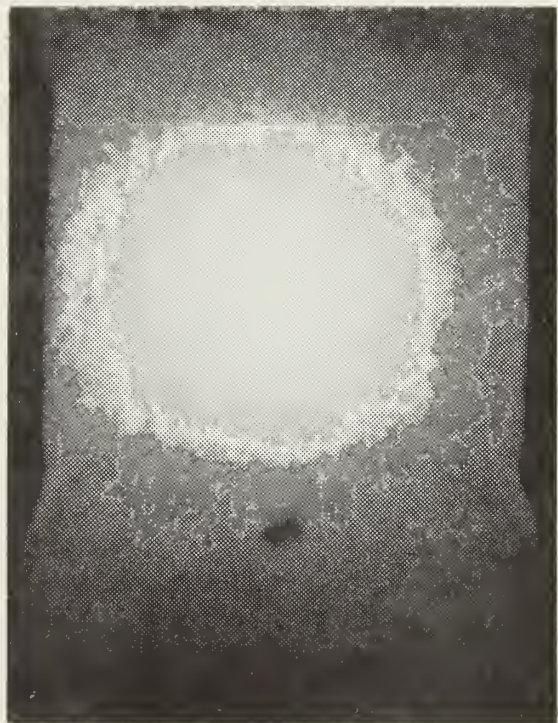
5



6

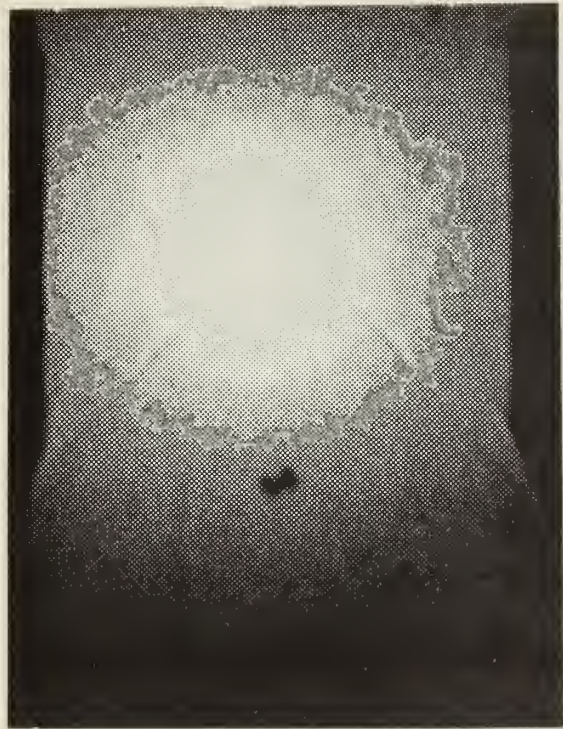


7

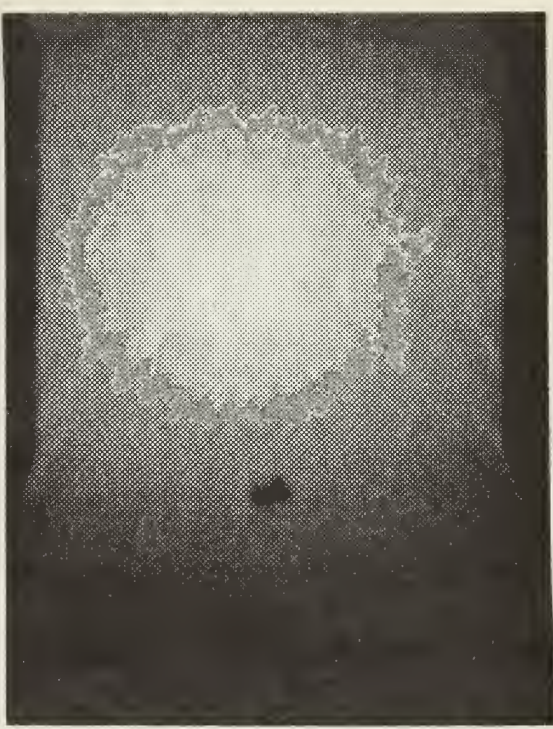


8

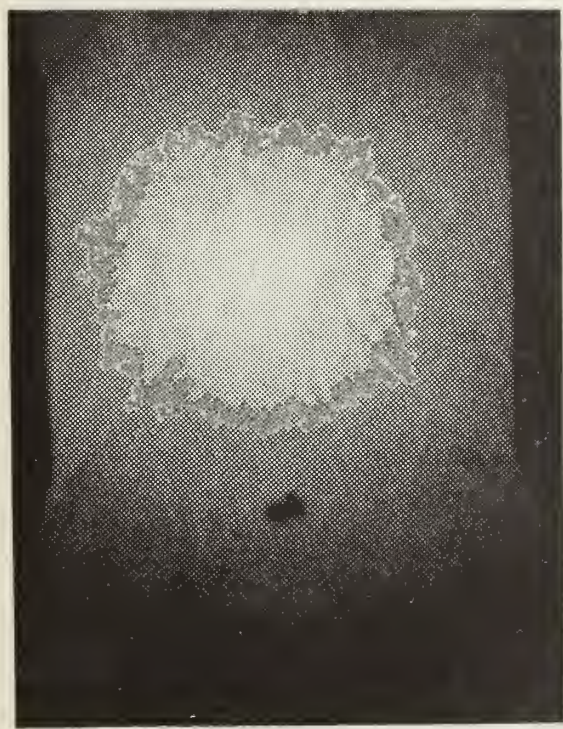
Figure 16. continued



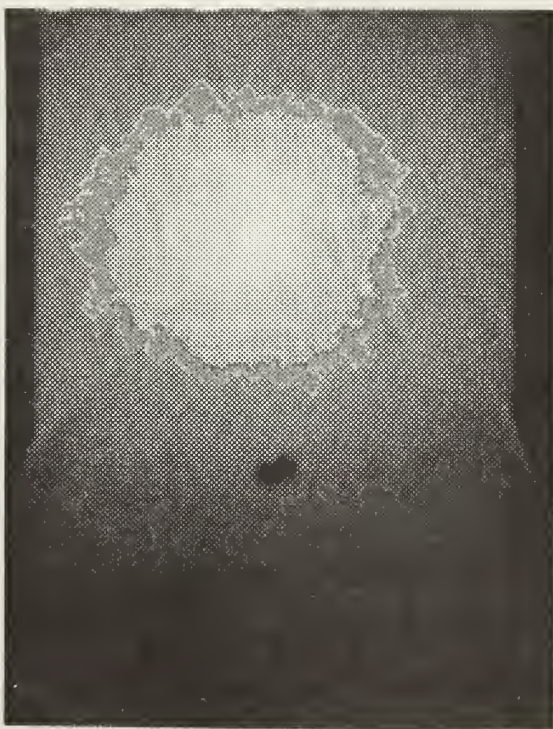
1



2



3



4

Figure 17. High speed sequence of steady condition.
Time between pictures in sequence, 0.28 ms.

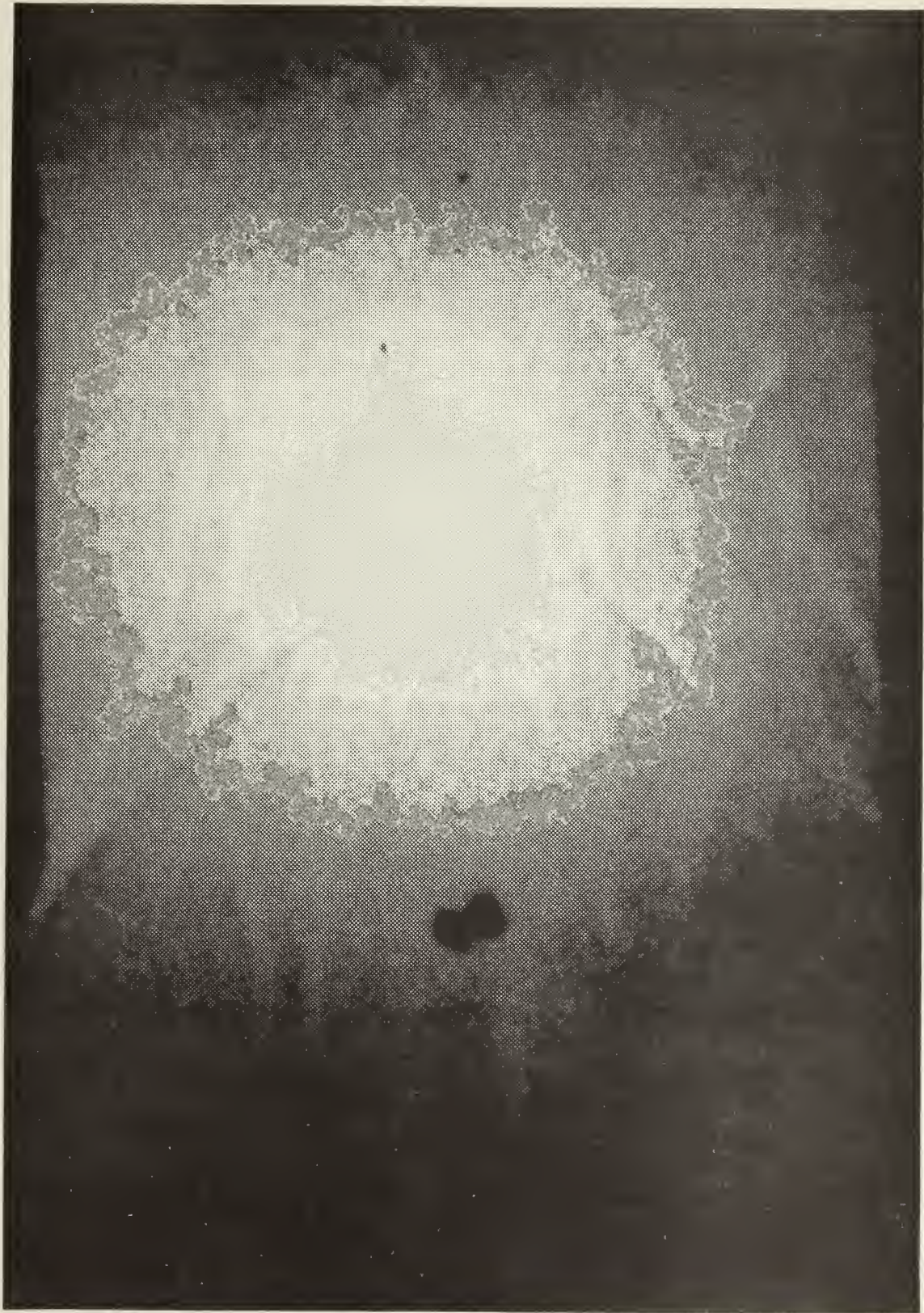


Figure 18. High speed shadowgraph of "bubble".

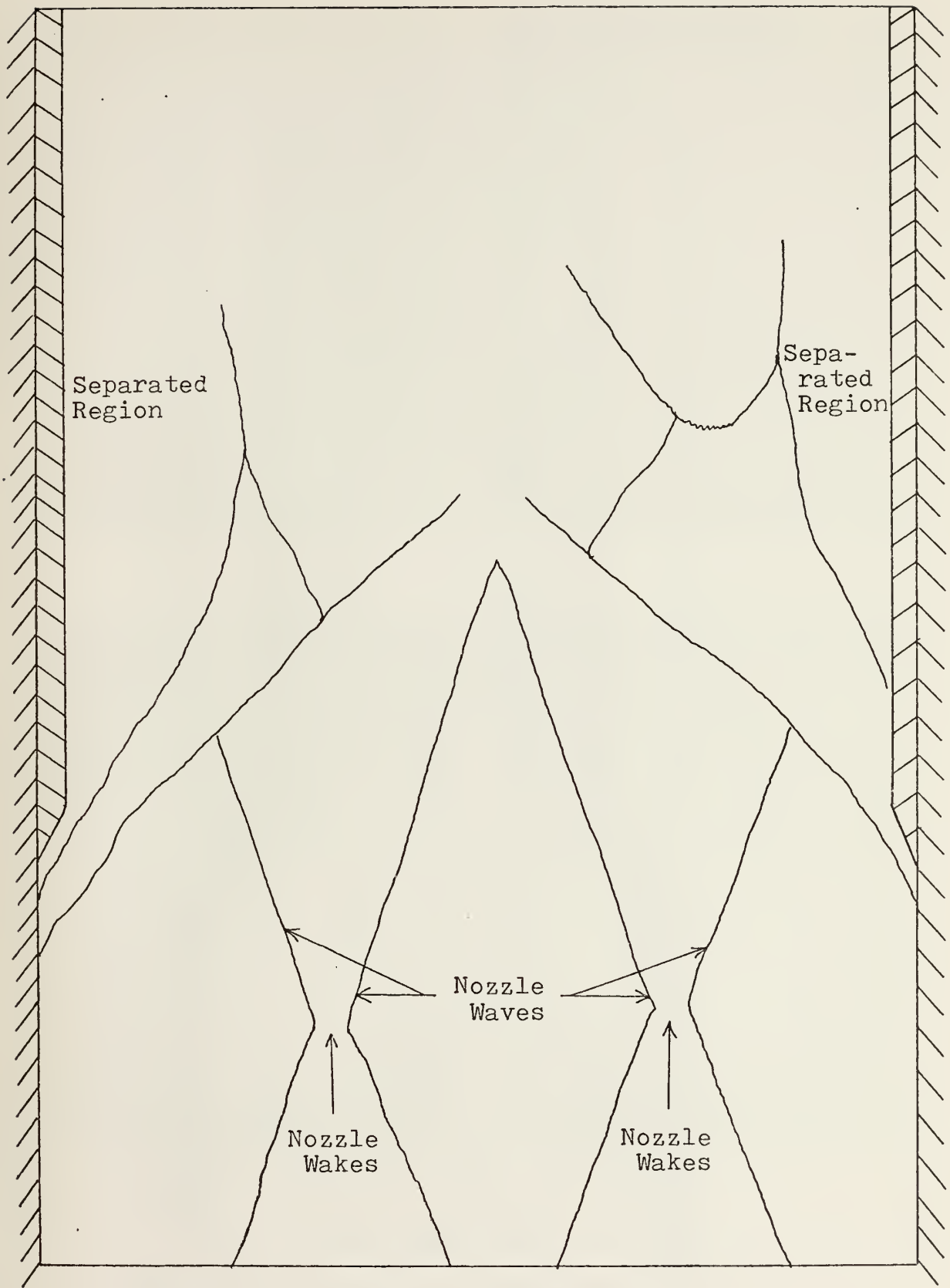


Figure 18a. Line trace of Shadowgraph.

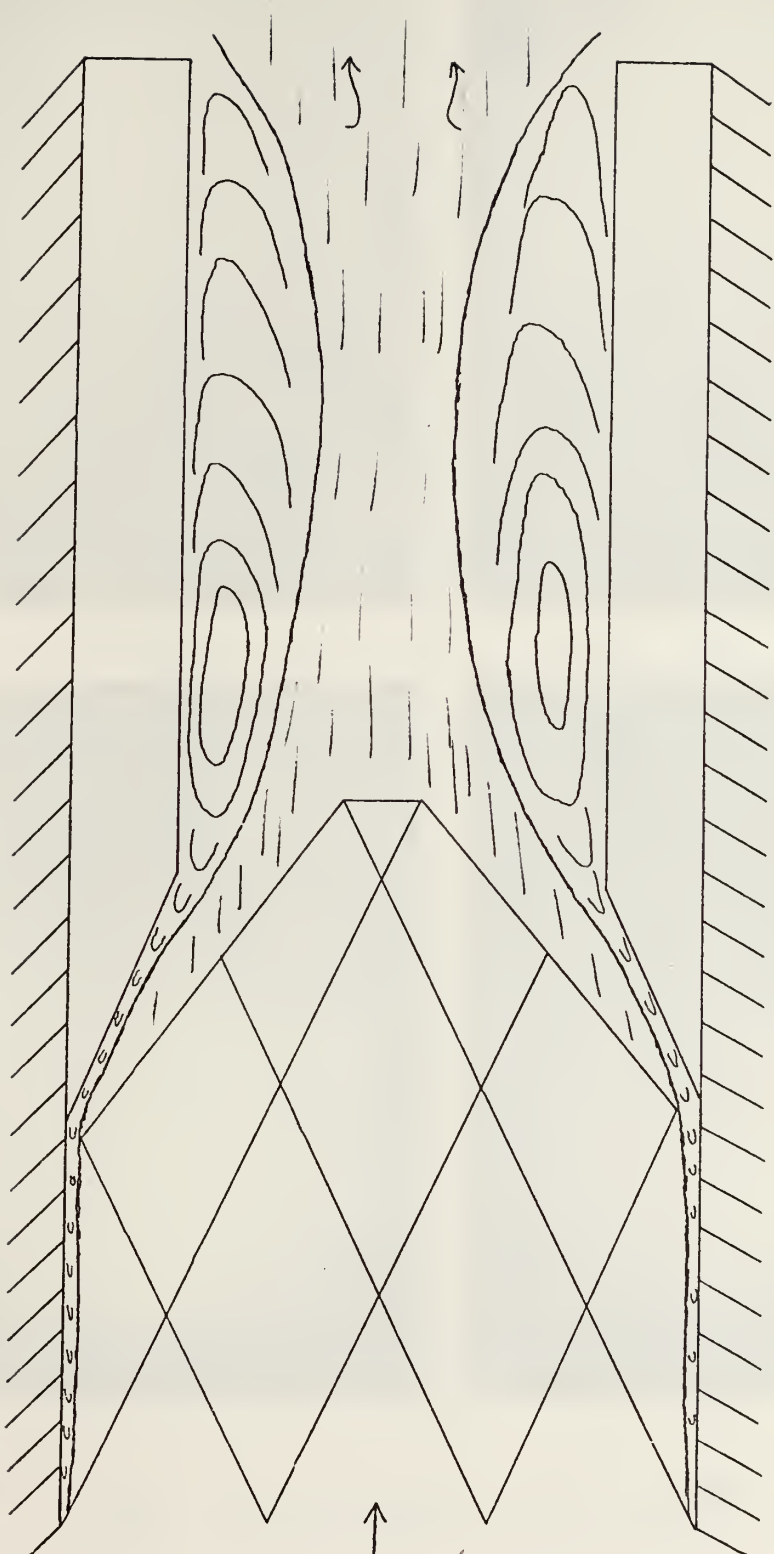


Figure 19. Diagram of "bubble" model.



1



2

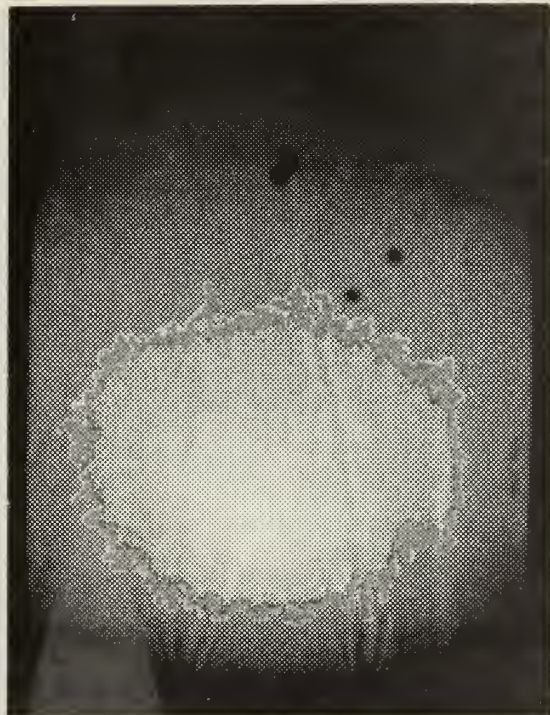


3

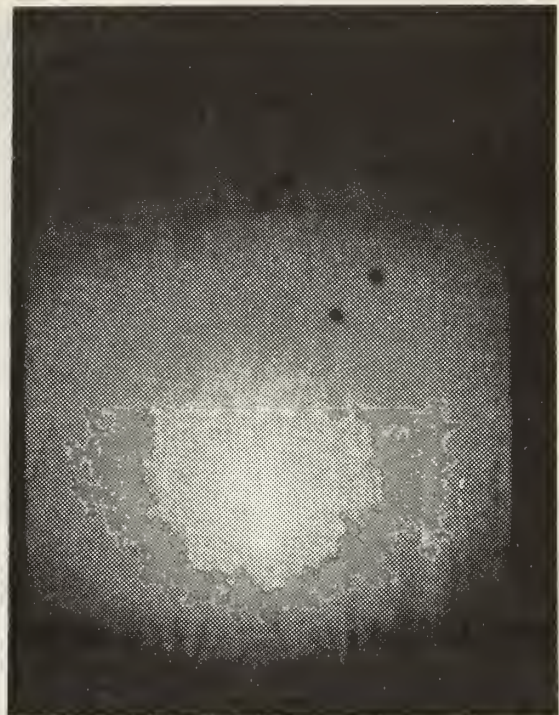


4

Figure 20. High speed sequence of the diffuser start process.
Time between pictures in sequence, 0.28 ms.



5



6



7



8

Figure 20. continued



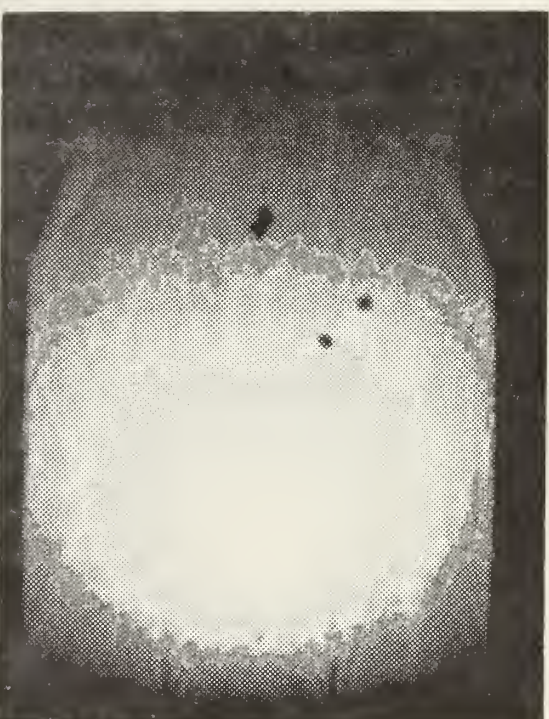
9



10



11



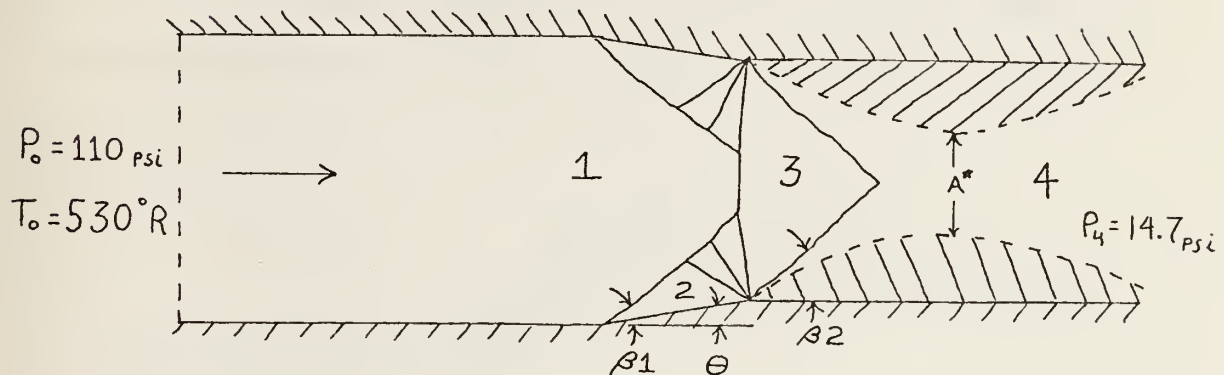
12

Figure 20. continued

APPENDIX A

CALCULATIONS OF SHOCK WAVE SYSTEM

I. Calculations showing the optimum position of the "bubble" and shock wave system.



A. Flow properties at position 1 were determined experimentally to be:

$$\begin{aligned} M_1 &= 4.0 \\ P_1 &= 0.73 \text{ psi} \\ T_1 &= 126^\circ\text{R} \end{aligned}$$

$$\begin{aligned} \beta_1 &= 43^\circ \\ \beta_2 &= 53^\circ \end{aligned}$$

B. Flow properties at position 2 were determined using oblique shock wave theory to be:

$$\begin{aligned} M_2 &= 1.96 \\ P_2 &= 6.18 \text{ psi} \\ T_2 &= 298^\circ\text{R} \end{aligned}$$

C. Flow properties at position 3 were determined using Prandtl Meyer expansion theory, with a turning angle of 19° to be:

$$\begin{aligned} M_3 &= 2.2 \\ P_3 &= 4.25 \text{ psi} \\ T_3 &= 268^\circ\text{R} \end{aligned}$$

D. Flow properties at position 4 were determined using oblique shock wave theory to be:

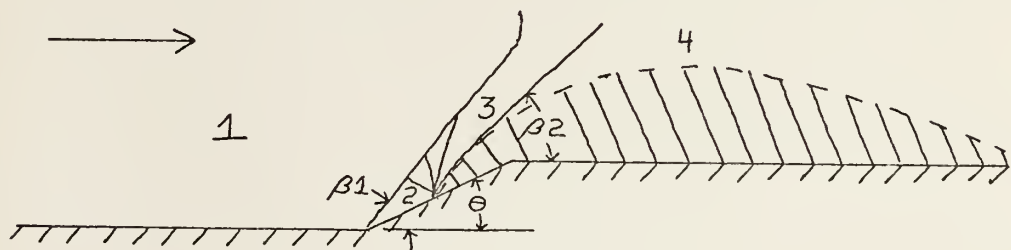
$$M_4 = 1.18$$

$$P_4 = 14.7 \text{ psi}$$

$$T_4 = 402^\circ R$$

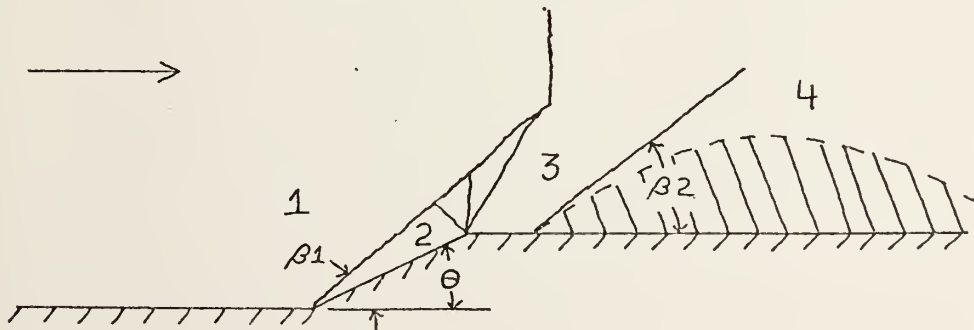
$A^* = 1.23$ inches (minimum for the second throat)

II. Diagram showing the "bubble" upstream from the optimum position.



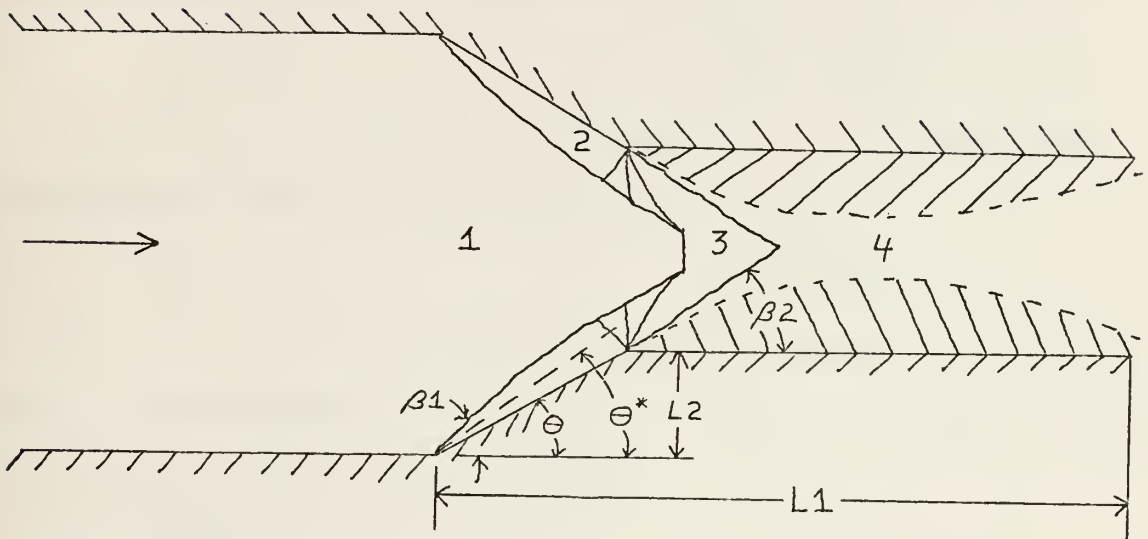
The same series of calculations as in section I were performed again. The only parameters changed were β_1, β_2 . In this case $\beta_1 = 55^\circ$, $\beta_2 = 63^\circ$. The area of the second throat (A^*) was calculated to be .892 inches, which was too small for the start sequence to begin.

III. Diagram showing the "bubble" downstream from the optimum position.



As in the previous sections, the calculations for the "bubble" downstream of the optimum position were performed in the same manner. In this case $\beta_1=39^\circ$, $\beta_2=48^\circ$. The area of the second throat (A^*) was calculated to be 1.45 inches, which was sufficient for a start sequence to begin.

APPENDIX B
PRELIMINARY DESIGN CALCULATIONS



$$L_1 = 4.5 \text{ inches}$$

$$L_2 = 0.35 \text{ inches}$$

$$\beta_2 = 54.72^\circ$$

$$M_1 = 4.0$$

$$T_{01} = 530^\circ R$$

$$\theta^* = \theta + 10^\circ$$

$$\theta = 10^\circ \text{ to } 30^\circ$$

$$\beta_1 \text{ variable}$$

In the first portion of the following plot, θ is varied from 10° to 30° and P_t is calculated (beginning with a fixed β_2) using oblique shock and expansion wave theory. In order to use the oblique shock charts directly and maintain 14.7 psi in section 4, it was necessary to introduce an empirical parameter, thus a factor of 10° was added to the turning angle θ . This 10° factor could be accounted for by such parameters as; 1) 3-D boundary layer effect shown in Ref. 9. 2) Incipient separation of boundary layers due to plane shock interactions stated in Ref. 9. 3) the build up of shocks at the base of the 19° ramp, causing the shock angle

to increase.

A sample of these calculations follow:

$$\beta_2 = 54.72^\circ \quad \theta = 19^\circ$$

A. Using the oblique shock wave theory, the flow properties for section 3 were determined to be:

$$M_3 = 2.65 \quad P_3 = 2.3 \text{ psi}$$

B. The flow properties for section 2 were determined using Prandtl Meyer expansion theory to be:

$$M_2 = 2.23 \quad P_2 = 5.0 \text{ psi}$$

C. The final calculations were for section 1, in which case it was necessary to add the 10° factor in order to use the oblique shock tables directly.

$$M_1 = 4.0 \quad P_1 = .66 \text{ psi}$$
$$P_t = 102 \text{ psi}$$
$$P_t/P_a = 6.9$$

The remaining points on the graph were obtained in the same way varying θ from 10° to 30° .

The second portion of this plot shows pressure recovery data taken from Ref. 4, which was obtained from laboratory results.

The correlation of the laboratory and calculated data is close although not exact, but as is shown in the plot, a "bubble" angle of 54.72° seems to be a close approximation to the actual angle of the "bubble" for Mach 4 flow.

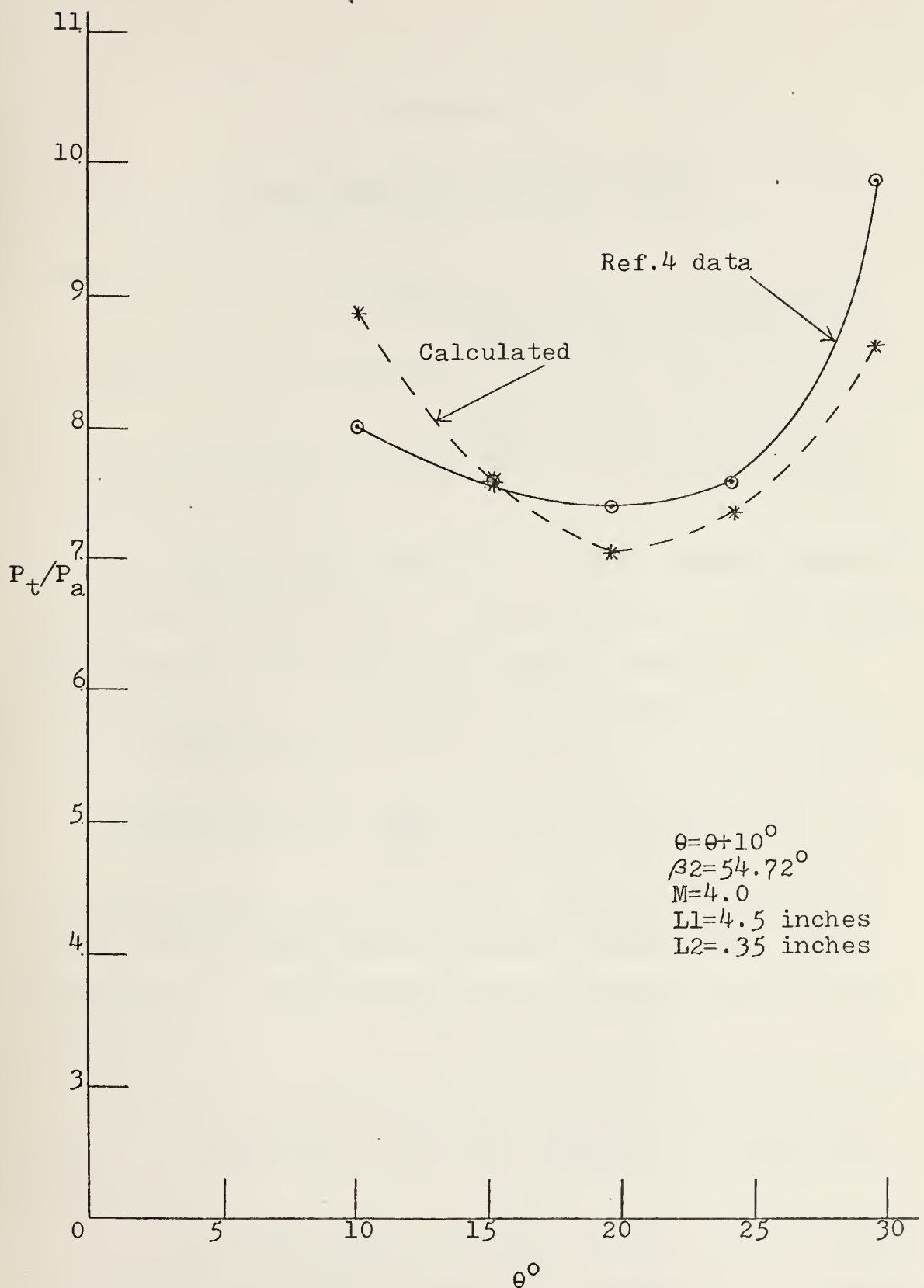
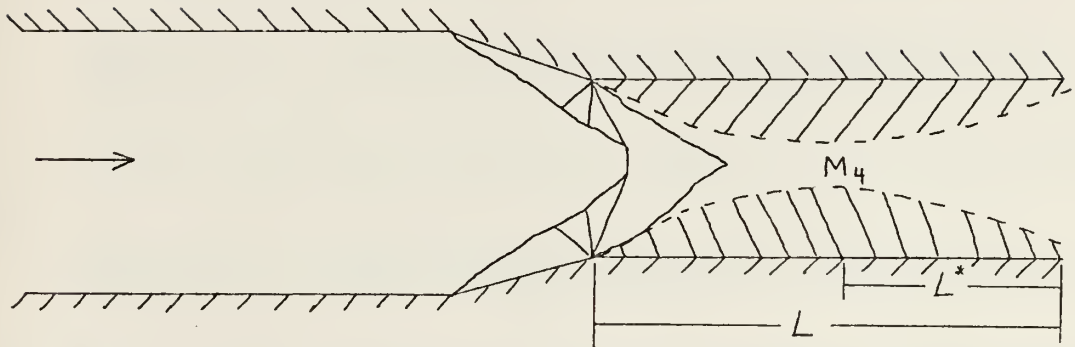


Figure 1B. Experimental and analytical plot of P_t/P_a for various θ .

APPENDIX C

CALCULATION OF FRICTION FACTOR



The above diagram shows the optimum "bubble" position. The length of the "bubble", (L) corresponds to the length of the diffuser. L^* is the half "bubble" length.

$$M_4 = 1.18 \quad (\text{obtained from Appendix A})$$

$$P_4 = 14.688 \text{ psi}$$

Using the formula $\frac{fL_{\max}}{D}$, a friction factor (f)

was calculated for the corresponding M_4 using a L_{\max} of 2.875 inches, which was determined from the high speed photographs. The hydraulic diameter (D) was taken to be 1.6 inches.

Using the above values, f was calculated to be 0.0156, which is a reasonable value when compared to those given in Ref. 8.

Note the compressibility effect on the friction factor as given in Fig. 13.10 of Ref. 3. For Mach 4 the compressible flow value is one half of the incompressible flow value.

LIST OF REFERENCES

1. AFWL Technical Report No. 71-83, Starting and Pressure Recovery in Fixed Throat Supersonic Diffusers, by T. Jones and S. Neice, 1972.
2. Shapiro, A.H., The Dynamics and Thermodynamics of Compressible Fluid Flow, Vol. I, Ronald Press, 1954.
3. Liepmann, W.H. and Roshko, A., Elements of Gasdynamics, p. 134, John Wiley and Sons, 1957.
4. Zerr, J.J., An Experimental Investigation of Short Diffusers for Gas Dynamic Lasers, M.S. Thesis, Naval Postgraduate School, 1974.
5. Aanerud, K.D., Analytical Investigation of Transient Diffuser Wave Phenomena, M.S.A.E. Thesis, Naval Postgraduate School, 1974.
6. Oriel Corporation of America, Operating Instructions, Universal Arc Lamp Sources, (2500 watts).
7. Ortwerth, J., report presented to Laser Diffuser Workshop held at NPS, 10-11 October 1974.
8. Shapiro, A.H., The Dynamics and Thermodynamics of Compressible Fluid Flow, Vol. II, Chapter 28, Ronald Press, 1954.
9. AIAA paper No. 74-0020, A Simple Correlation for Incipient Turbulent Boundary-Layer Separation due to a Skewed Shock Wave, by R.H. Korkegi.
10. NAVORD Report 1570, Diffuser Investigation in a Supersonic Wind Tunnel, by J.L. Diggins, 1951.
11. AIAA paper No. 69-447, A Two Dimensional Mixed Compression Inlet System Designed to Self Restart at a Mach Number of 3.5, by W.E. Anderson and N.D. Wong.
12. NACA technical Note 3545, Investigation of the Effect of Short Fixed Diffusers on Starting Blow Down Jets in Mach Number range of 2.7 to 4.5, by J.A. Moore, 1956.
13. Reneau, L.R., Johnston, J.P., and Kline, S.J., "Performance and Design of Straight, Two-Dimensional Diffusers".

14. Rotty, R.M., Introduction to Gas Dynamics, Wiley and Sons, 1957.
15. John, E.A.J., Gas Dynamics, Allyn and Bacon, Inc., 1969.
16. Schichting, H., Boundary Layer Theory, McGraw Hill, 1968.
17. ARL technical Report No. 73-0137, Shock Wave-Turbulent Boundary Layer Interaction in Hypersonic Flow, by M.S. Holden, 1973.
18. NACA technical Memorandum X-3026, Comparison of Theoretical and Experimental Boundary-Layer Development in a Mach 25 Mixed-Compression Inlet, by W.R. Hingst and C.E. Towne, 1974.

INITIAL DISTRIBUTION LIST

	No. Copies
1. Defense Documentation Center Cameron Station Alexandria, Virginia 22314	2
2. Library, Code 0212 Naval Postgraduate School Monterey, California 93940	2
3. Department Chairman, Code 57 Department of Aeronautics Naval Postgraduate School Monterey, California 93940	2
4. Assoc Professor O. Biblarz, Code 57 Zi (thesis advisor) Department of Aeronautics Naval Postgraduate School Monterey, California 93940	3
5. Professor A.E. Fuhs, Code 57 Fu Department of Aeronautics Naval Postgraduate School Monterey, California 93940	1
6. Dr. James Ortwerth AFWL Kirtland Air Force Base New Mexico 87117	1
7. LCDR Milford M. Oudekerk, USN (student) NAVPLANTREP Lockheed Aircraft Corporation Burbank, California 63282	1
8. Mr. William Volz, Code 320 Naval Air Systems Command Washington, D.C. 20360	2

161381

Thesis

09

c.1

Oudekerk

Experimental investi-
gation of the starting
process of short dif-
fusers for gas dynamic
lasers.

161381

Thesis

09

c.1

Oudekerk

Experimental investi-
gation of the starting
process of short dif-
fusers for gas dynamic
lasers.

thes09
Experimental investigation of the starti



3 2768 001 97418 1
DUDLEY KNOX LIBRARY